Energy & Buildings 342 (2025) 115852

Contents lists available at ScienceDirect

Energy & Buildings

journal homepage: www.elsevier.com/locate/enb

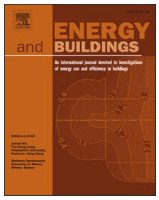

Refining climate zoning in North Africa: A 30-Year analysis of heating and cooling degree days for energy planning and adaptation

Mohamed Elhadi Matallah [a,b,*], Andreas Matzarakis [c,d], Aissa Boulkaibet [e], Atef Ahriz [f], Dyna Chourouk Zitouni [a], Fatima Zahra Ben Ratmia [g], Waqas Ahmed Mahar [a,h], Faten Ghanemi [i], Shady Attia [a]

[a] Sustainable Building Design Lab, Department UEE, Faculty of Applied Sciences, University of Liège, Belgium
[b] Civil Engineering and Hydraulics Laboratory, Sustainable Development and Environment (LARGHYDE), University of Biskra, Algeria
[c] Chair of Environmental Meteorology, Faculty of Environment and Natural Resources, University of Freiburg 79085 Freiburg, Germany
[d] Democritus University of Thrace, GR-69100 Komotini, Greece
[e] Laboratory Evaluation of Quality of Use in Architecture and the Built Environment, University of Oum el Bouaghi, Algeria
[f] Department of Architecture, Echahid Cheikh Larbi Tebessi University, Algeria
[g] Laboratory of Design and Modelling of Architectural and Urban Forms and Ambiances (LACOMOFA), University of Biskra, Algeria
[h] Department of Architecture, School of Art, Design and Architecture (SADA), National University of Sciences and Technology (NUST), Islamabad 44000, Pakistan
[i] Department of Architecture, Mohamed Khider University, Biskra, Algeria

ARTICLE INFO

Keywords:
Köppen-Geiger classification
Data Access Viewer (DAV)
HDD
CDD
GIS
Spatial Distribution

ABSTRACT

This research investigates the spatial variability of heating degree days (HDD) and cooling degree days (CDD) to advance climate zoning across North Africa. Using 30 years of high-resolution meteorological data (1989–2019) from 108 weather stations in Egypt, Libya, Tunisia, Algeria, Morocco, and Western Sahara, HDD and CDD values were calculated for six base temperatures (HDD: 12 °C–22 °C; CDD: 18 °C–28 °C) using NASA/POWER data. The findings reveal substantial climatic and topographical influences on thermal energy demands. Northern regions, particularly high-altitude locations like Bordj Bou Arreridj, Algeria, exhibited the highest HDD values, reaching 2932 at 18 °C, while southern desert areas, such as Adrar, Algeria, demonstrated extreme CDD values, peaking at 3169 at 18 °C. GIS-based spatial interpolation methods enhanced visualization, delineating detailed sub-classifications within the Köppen-Geiger framework, increasing spatial resolution from 12 321 km2 to 3025 km2. For example, Algeria alone expanded from five to 35 sub-classifications. These refined zones reveal critical differences in energy demand, with northern cities requiring up to 10 times more heating energy, while southern cities demand up to eight times more cooling energy compared to coastal zones. The results provide an essential basis for updating regional building codes and optimizing HVAC designs, supporting climate adaptation and energy efficiency strategies tailored to North Africa's diverse climatic zones. By enhancing spatial resolution and refining classifications, this research transforms energy planning and thermal regulations in the region.

Abbreviations: ASHRAE, American Society of Heating, Refrigerating, and Air-Conditioning Engineers; BSh, Hot semi-arid climate; BSk, Cold semi-arid climate; BWh, Hot desert climate; BWk, Cold desert climate; CDD, Cooling Degree Days; Cfa, Humid subtropical climate; Csa, Hot-summer Mediterranean climate; Csb, Warm-summer Mediterranean climate; CSV, Comma-Separated Values; DTR C3-3, Algerian Thermal Regulation Code; EPW, EnergyPlus Weather file format; GIS, Geographic Information Systems; HBRC, Housing and Building National Research Centre (Egypt); HDD, Heating Degree Days; HVAC, Heating, Ventilation, and Air Conditioning; IPCC, Intergovernmental Panel on Climate Change; KGC, Köppen-Geiger Climate classification; MODIS, Moderate Resolution Imaging Spectroradiometer; NASA/POWER, Prediction of Worldwide Energy Resources; NOAA, National Oceanic and Atmospheric Administration; RTCM, Regulatory Thermal Code in Morocco; TMY, Typical Meteorological Year file; WMO, World Meteorological Organization; WHO, World Health Organization.

* Corresponding author.
E-mail addresses: elhadi.matallah@univ-biskra.dz (M.E. Matallah), andreas.matzarakis@meteo.uni-freiburg.de (A. Matzarakis), Aissa.boulkaibet@univ-oeb.dz (A. Boulkaibet), atef.ahriz@univ-tebessa.dz (A. Ahriz), dyna.zitouni@student.uliege.be, dynachourouk.zitouni@univ-biskra.dz (D.C. Zitouni), fatimazahra.benratmia@univ-biskra.dz (F.Z. Ben Ratmia), waqas.mahar@sada.nust.edu.pk (W.A. Mahar), faten.ghanemi@univ-biskra.dz (F. Ghanemi), shady.attia@uliege.be (S. Attia).

https://doi.org/10.1016/j.enbuild.2025.115852
Received 13 January 2025; Received in revised form 1 May 2025; Accepted 7 May 2025
Available online 10 May 2025

1. Introduction

Climate classification systems, particularly the Köppen-Geiger climate classification (KGC) system published in 1884, provide a structured approach to categorizing global climates [1,2,3]. These systems can be either empiric (based on observed features) or genetic (considering underlying causes) (Table 1), and serve to identify climatic patterns and stimulate research [4,5]. With climate change becoming an increasingly critical concern [6], organizations like the Intergovernmental Panel on Climate Change (IPCC) have documented its widespread impacts through comprehensive assessments and reports [7]. Nowadays, satellite technology has revolutionized climate monitoring, notably measuring sea level rise and Arctic ice decline [8]. Modern satellite systems have become essential for collecting global climate variables such as temperature, humidity, and wind speed [9,10]. In fact, key NASA missions include:

- AIRS (Atmospheric Infrared Sounder) for temperature and humidity profiling [11].
- MODIS for land surface temperature measurement [12].
- AMSR2 for sea surface wind speed monitoring [13].

These data are managed through NASA's EOSDIS and its DAACs, providing near real-time access for various climate research applications [14,15].

Climate change is widely recognized as one of the primary environmental challenges facing the planet. According to Zhai and Helman, 2019 [16], buildings account for approximately 30 % of global annual greenhouse has (GHG) emissions and consume up to 40 % of all energy between 1970 and 2004, as reported by the IPCC [7]. Improving energy efficiency in buildings plays a crucial role in achieving the ambitious goal of carbon-neutrality by 2050, and considered a key factor in evaluating sustainable living spaces [17]. Moreover, building energy consumption, particularly for space cooling and heating, is directly affected by climate change [18]. In response to building climate adaptation, degree days are fundamental metrics for evaluating building energy demand and performance in relation to climate variations [19,20]. This concept encompasses both heating degree days (HDD) and cooling degree days (CDD), calculated as the difference between daily average temperature and a baseline of 65 °F (18 °C). The U.S. Department of utilizes these metrics to help estimate energy consumption and costs [21,22]. Climate Change impact on degree days has been documented in several studies. Spinoni et al, 2018 [23] demonstrated decreasing HDDs and increasing CDDs across Europe from 1981 to 2100, while Petri and Caldeira, 2015 [24] projected that U.S. cities will experience degree day patterns similar to current southern climates by century's end. Recent studies, including those using machine learning models, have shown that seasonal and long-term changes in surface temperature are closely linked to variations in heating and cooling degree days, highlighting the need for spatial temperature modeling to better estimate energy demand [25,26]. Additionally, studies analyzing spatial and temporal temperature patterns have shown in land characteristics significantly affect localized thermal variations [27], which can influence long-term heating and cooling degree day trends used in energy planning models.

These changes have broader implications for thermal comfort, building design, and socioeconomic factors [20,28,29]. Long-term studies have shown that changes in surface temperature are linked to variations in heating and cooling degree days, showing the need for spatial temperature models to better estimate energy demand [30]. Furthermore, in agricultural applications, Growing Degree Days (GDDs) serve a different purpose, measuring the heat accumulation required for plant maturity, helping determine optimal cultivation locations and timing [31,32].

Indoor environmental quality has become a key policy focus due to its significant impact on human health [33,34]. ASHRAE 55–1992 standards recommend specific optimal temperatures (22 °C in winter, 24.5 °C during summer) for sedentary activities [35], while issues like fuel poverty in the UK [33] and indoor overheating in southern European countries such as Portugal and Greece [36,37] highlight the challenges of maintaining thermal comfort.

Africa faces particularly severe challenges in housing market and thermal comfort. The continent experiences widespread fuel poverty and substandard heating and cooling systems [38]. Urban challenges are compounded by extensive informal housing, with UN-Habitat reporting 535 million Africans living in slum condition as of 2012 [39,40]. These housing market issues stem from multiple factors, including rapid urbanization, inappropriate policy and regulatory frameworks, dysfunctional housing markets, and a lack of political will [38]. While Africa's construction sector lags behind global standards, potential solutions include developing informal construction sectors and innovative housing finance systems [38,41]. However, experts caution against oversimplified approaches that focus solely on reducing construction costs.

In the light of these challenges, the building energy management in Africa faces multiple critical issues. The continent urgently requires crucial policies addressing heating or cooling systems to ensure basic livability conditions for its population. Addressing these requirements necessitates a thorough understanding of existing infrastructure gaps and the development of detailed building energy demands maps. Such analysis would provide a foundation for evidence-based policy making and targeted interventions to improve living conditions across the continent.

Thus, the energy consumption for heating and cooling, whether from diesel fuel or electricity, largely depends on the local climate conditions and seasonal variations. HDD and CDD are crucial metrics for analyzing and regulating building energy demands and insulation. These factors help determine the energy requirements needed to maintain comfortable indoor temperatures throughout the year, particularly in the African regions.

Given the complex interplay between climate variability, building conditions, and energy demands, the current study seeks to bridge critical knowledge gaps in understanding new climate classifications related to housing challenges, by integrating climate data, degree day analysis, and spatial distribution of the HDDs and CDDs values, we aim to explore the multifaceted dimensions of real climate zoning requirements, particularly in North Africa that experiencing rapid urbanization and significant climatic transitions. The research aims to refine a novel classification of climate zoning in North Africa based on a 30-year analysis of HDDs and CDDs variations. In this regard, the objective of this paper is an attempt to respond to the following research questions:

- Does the current Köppen-Geiger Climate classification (KGC) accurately represent the existing climate zones in North Africa?
- How can Heating and Cooling Degree Days serve as accurate tools for redrawing new climate zones for building energy standards in North African territories?

By answering the questions above, this paper provides a critical overview of the climate zoning reality in North Africa based on a 30-year analysis of the Heating Degree Days (HDDs) and Cooling Degree Days (CDDs) criteria. The paper's novelty is an exhaustive study that takes into account several geographical and climatic parameters that are ignored by the Köppen-Geiger Climate Classification (KGC), such as altitude and ambient temperatures. Five African countries and one territory were investigated within 108 weather stations. A new climate mapping was developed based on the calculation of the HDDs and CDDs over 30 years. An accurate spatial distribution was done via a GIS model of the newly developed climate sub-classifications of the North African region. To the best of our knowledge, this is the first paper that provides relevant insights into the heating, ventilation, and air-conditioning (HVAC) requirements of buildings and their actual spatial distribution in North Africa. The originality of the paper is twofold. First, the paper

Table 1
Relevant studies regarding different climate classifications and their experimental methods.

References	Study period	Context	Analyzed parameters	Research method
Strohmenger et al., 2024 [42]	– Historical period 1976–2005 – Future period 2070–2099	Distinct parts of France	– Average annual and monthly air temperature – Precipitation	Simulation with ADAMONT and CDF-t for calibrating climate model
Phumkokrux et al., 2024 [45]	Historical period 1987—2021	Thailand	– Mean annual air temperature – Annual rainfall and evaporation	New Thornthwaite climate classification method
Andrade et al., 2023 [43]	– Period 1970–2000 – Future period 2041–2060	World map	– Monthly precipitation max, min and average temperatures. – WorldClim data	Using GCMs (Global Climate Models) as simulation models for predicting future climate pattern
Hobbi et al., 2022 [2]	– Historical period 1980–2017	Different regions around the world	– Precipitation and temperature data.	– Evaluating 7 global datasets to investigate uncertainties in the Köppen-Geiger (KGC). – Analyzing spatially the differences in the KGC maps
Valjarević et al., 2022 [44]	Future period 2081—2100	4261 meteorological stations in the world	Global temperatures and precipitation patterns	– Used climate models – Analyzed 4261 meteorological stations for temperature and precipitation data predicted
Cui et al, 2021 [1]	– Historical period 1979–2013 – Future period 2020–2099	Different regions around the world	12 bioclimatic variables including temperature and precipitation.	– Using multiple observational datasets to derive historical Koppen-Geiger climate classification maps – Using a set CMIP5 (Coupled Model Intercomparison Project Phase 5) for future climate maps
McCurley and Pisarello, 2021 [46]	Historical period 1980–2018	All regions of the world, except Antarctica.	Evapotranspiration rate and precipitation	– Developed three new classification systems based on evapotranspiration rates and precipitation.

calculates the heating and cooling demands for 108 cities in North Africa over 30 years. Secondly, the paper develops a new climate zoning mapping for this region which can be adjusted to the Köppen-Geiger Classification to determine building energy needs, specifically for housing within this region. The paper identifies new climate sub-classifications that local policies can apply to maintain near-optimal sustainability for building energy demands. Finally, it provides a concrete set of recommendations that can serve as tools to address the climatic and socio-economic variability of people in the region.

2. Literature review

2.1. Climate classification methods

Despite numerous studies on worldwide climate zoning, most focus on observed or future projections to define climate change impacts. Otherwise, studies on heating and cooling demands for climate zoning remain very limited.

In the context of climate zoning methodologies, Strohmenger et al, 2024 [42] conducted a study on the Köppen-Geiger climate classification across France, utilizing a set of high-resolution climate projections. They employed 84 future projections from 1976 to 2099. The study anticipates moderate changes in climate types by 2035 for approximately 20 % of France. However, significant changes are projected after 2040 under the RCP 8.5 scenario, affecting 86 % of France, with a notable expansion of temperate climates, including hot summers, extending into mountainous regions. In another context, Andrade et al, 2023 [43] investigated worldwide Köppen-Geiger Climate classification changes. The study projects significant shifts in global climate zones under two emission scenarios: SSP2-2.6 (low emissions) and SSP5-8.5 (high emissions). By mid-21st century (2041–2060), polar climates are expected to shrink, particularly tundra and icecap zones, while hot desert, semi-arid, and humid subtropical climates are projected to expand. These findings emphasize the dynamic nature of climate zones and the importance of mitigating greenhouse gas emissions to manage future climate impacts. Furthermore, Hobbi et al, 2022 [2] investigated the uncertainties in the Köppen-Geiger climate classification by analyzing seven global gridded datasets of precipitation and temperature over the period 1980–2017. The study highlights significant discrepancies in climate classification maps due to differences in data sources. Key findings include 17 % of grid points showing variations in major climate types and strong uncertainties in regions like South Asia, Africa, and parts of the Americas. The study proposes two robust master climate maps by combining all datasets, offering improved spatial consistency and helping to evaluate historical and future climate shifts better.

Valjarević et al, 2022 [44] updated the Köppen-Geiger Trewartha Climate Classification (TWCC) to analyze global climate changes using four climate change scenarios (RCP2.6, RCP4.5, RCP6.0, and RCP8.5) for the period 2021–2100. By employing GIS-based spatial analysis, the study projects significant shifts in climate zones due to temperature increases between 0.3 °C and 4.3 °C. Major changes are expected in Australia, Southeast Asia, South America, and North America, with tropical and arid climates (e.g., BWh, BSh) showing notable transformations.

Cui et al. 2021 [1] investigated observed and projected changes in global climate zones using the Köppen Climate Classification. The study highlights significant shifts in climate zones due to anthropogenic global warming. Observations since the 1980 s show a notable expansion of hot tropics and arid climates into middle and high latitudes, while polar zones shrink due to accelerated Arctic warming. Projections indicate continued poleward and upward shifts in climate zones under future warming scenarios, with uncertainties remaining in the rate and scale of these changes. The findings emphasize the profound ecological impacts, such as shifts in species ranges and biome distributions, resulting from climate zone changes.

In another context, Phumkokrux and Trivej, 2024 [45] examined the impacts of climate change and agricultural diversification on the agricultural production value of Thai farm households. The study projects that even if global warming is limited to 1.5 degrees Celsius, rising temperatures will continue to impact agricultural production in Thailand under various IPCC scenarios. When McCurley et al, 2021 [46] evaluated global hydroclimate classification systems, focusing on coherence and simplicity. The study compares four established systems, including Köppen–Geiger, with four newly proposed. The Water-Energy Clustering (WEC) system is highlighted for its improved coherence in key variables like precipitation and evapotranspiration while reducing complexity by using two parameters. WEC outperforms traditional systems in defining uniform zones, making it suitable for large-scale water resource management. The study underscores the need for tailored frameworks to enhance hydroclimate analysis and policy applications.

2.2. Global mapping of the heating and cooling degree days

The mapping of heating and cooling degree days has been conducted in various studies worldwide, though coverage remains geographically limited across several continents.

Al-Hadhrami., 2013 [47], conducted a comprehensive analysis calculating and mapping the CDD and HDD across Saudi Arabia using long-term temperature data from 38 meteorological stations. It identified the variations in energy demand for cooling and heating across different regions. While the study provides valuable insights into regional energy requirements and can assist in designing energy-efficient systems, estimating energy consumption, it relies on a single base temperature of 18.3 °C for all regions, potentially limiting its accuracy in reflecting local energy needs. In Pakistan, Amber et al, 2018 [48] analyzed HDD/CDD values for 22 cities using 30 years of temperature data. Their mapping efforts established an important baseline for energy forecasting and building energy efficiency planning [49]. However, the limited number of cities studied restricts the generalization of findings across the entire country.

In Europe, Spinoni et al, 2015 [50], developed comprehensive climatologies and trends mapping for HDD, CDD, and Growing Degree Day (GDD) across Europe. Their 60-year analysis revealed significant decreases in HDD and increases in CDD, providing critical insights into climate-induced changes in energy consumption and agricultural production. While the study was validated using independent datasets, the spatial interpolation methods employed could introduce errors in regions with sparse data coverage. The Pan-European Thermal Atlas (PETA) by Möller et al, 2018 [51] represents a significant advancement in mapping heating and cooling demands across Europe. This study integrates geospatial data to identify heat demand densities, potential district heating areas, and optimal supply zones. While the atlas enables sophisticated analysis of local energy mixes and cost-effective district heating strategies. However, its methodology heavily depended on heating demand data availability and quality, which varies significantly across regions. Janković et al, 2019 [52] conducted a detailed assessment of climate change impacts on residential heating and cooling energy demands in Serbia using regional climate modeling (RCM) under A1B and A2 scenarios. The research analyzed HDD and CDD over four periods (1971–2000, 2011–2040, 2041–2070, and 2071–2100) to project spatial and seasonal changes in energy requirements. The findings revealed a significant decrease in HDDs, particularly in southern Serbia, and an increase in CDDs, most pronounced in northern Serbia. The analysis projects that by the century's end, the traditional HDD to CDD ratio will shift substantially, with cooling demands becoming increasingly dominant in the overall energy consumption pattern. While, these results offer crucial insights for energy management, policy development, and building energy efficiency strategies in Serbia, it has notable limitations. The study's geographical scope is restricted to Serbia, Potentially limiting its broader regional applicability. Additionally, the use of fixed base temperatures (19 °C for HDD and 18.3 °C for CDD) does not account for variations in building designs, insulation, or user behaviors.

Azimi et al, 2020 [53] investigated climate change impacts on energy demand in the southern Caspian Sea region, analyzing HDD and CDD from simulated temperature data between 2015 and 2050 under the A1B climate scenario. Using the EH5OM model and RegCM4 for downscaling, they established relationships between temperatures metrics and geographical factors such as elevation, latitude, and longitude. Their findings showed that higher elevations correlate with lower CDD and higher HDD values. However, the study's use of fixed base temperatures (18.3 °C for HDD and 23.9 °C for CDD) may not accurately reflect the diverse comfort requirements across different building types and socioeconomic contexts. Moreover, the study of Andrade et al, 2021 [54] analyzed the impact of climate change on HDD and CDD demands for residential in Portugal. It employed climate projections from EURO-CORDEX under RCP4.5 and RCP8.5 scenarios to forecast energy needs for the periods 2011–2040 and 2041–2070, compared to a historical baseline (1971–2000). The study identified a significant decrease in HDDs and an increase in CDDs, highlighting shifting energy demands toward cooling, particularly under RCP8.5. The study provided spatial distribution of energy demand variations, offering critical insights for energy planning, building design, and policy adaptation in the context of climate change. However, the study assumed fixed base temperatures for HDD (18 °C) and CDD (25 °C), which may not account for varying building types, user behaviors, and thermal comfort thresholds.

In U.S., Fry, 2021 [55] introduced an innovative method to mapping building heating demand for district heating planning in Montana, Idaho, and Washington. The study overcomes proprietary utility data limitations by utilizing open-source imagery, and energy consumption surveys. While the research provides valuable tools for techno-economic evaluations and building stock decarbonization through Comsof Heat simulation software, its geographic scope remains limited to select municipalities.

From a global perspective, Li et al, 2021 [56] analyzed the spatial–temporal distribution and changes in global HDDs over a 49-years period (1970–2018). The study revealed significant correlations between HDDs and determinants such as latitude, altitude, mean albedo, vegetation indices, and pollution levels (PM2.5). Through machine learning approaches, the research developed models to predict HDDs and their inter-annual variation patterns. The findings highlighted global trends influenced by climate change, providing valuable insights for energy planning, urban development, and climate adaptation strategies. Moreover, Miranda et al, 2023 [57] conducted a global analysis examining the impact of warming from 1.5 °C to 2.0 °C on CDDs worldwide using an extensive ensemble of 2,100 high-resolution simulations. The study showed significant geographical variations in projected cooling demand increase, with two particularly notable patterns: Sub-Saharan Africa showed the highest absolute increases in cooling demands, while traditionally cooler regions such as Switzerland and the UK demonstrated the most dramatic relative increases. The research identified critical implications for global energy management and climate adaptation. In Sub-Saharan Africa, the substantial increase in CDD highlights the urgent need for infrastructure development and energy access improvements. These findings emphasize the critical importance of limiting global temperature rise, as even the difference between 1.5 °C and 2.0 °C scenarios shows substantial impacts on energy demands and heat exposure. The study underscores the necessity of targeted adaptation strategies that consider both absolute and relative changes in cooling demands across different geographical and socio-economic contexts.

Research on spatial distribution of heating and cooling building demands in Africa remains notably limited, with existing studies primarily focusing on local conditions rather than comprehensive regional analysis.

In Morocco, Idchabani et al, 2013 [58] conducted a comprehensive evaluation and mapping of HDD and CDD using data from 37 weather stations spanning 2000–2009. The methodology incorporated multiple base temperatures to effectively represent Morocco's six distinct climatic zones. The researchers developed regression models to estimate degree-days in regions lacking weather stations by analyzing the relationships between degree-days and geographical factors including elevation, latitude, and longitude. The resulting maps and analytical models provide architects and engineers with essential tools for estimating building energy consumption, optimizing energy-efficient designs, and properly sizing HVAC systems. However, the study's limitations include its geographic restriction to Morocco rather than encompassing the broader North African region, and its reliance on a relatively short 10-year dataset, which may not capture long-term climatic patterns and trends. In South Africa, Conradie et al, 2018 [59] developed improved climatic maps for South Africa to better support energy-efficient building design. Their study critiqued the inadequacy of the existing six-zone climate map in the SANS 204 building standard,

using 21 years of climatic data and climate change projections to map HDD and CDD quantities. While these maps demonstrated correlation with modeled building energy demand, the Standard Effective Temperature (SET) map, incorporating humidity and dry-bulb temperature, showed poor correlation with annual building heating and cooling energy demands. Semahi et al, 2020 [60], combined building performance simulations and GIS to create high-resolution spatial maps of discomfort hours and energy needs for 74 Algerian cities. While their research supports sustainable urban planning and building design through identification of energy demands patterns, it remains localized and does not update Algeria's existing climate zones. In another context, Dicko et al, 2024 [61] conducted a detailed analysis of CDDs trends in two major West African cities: Kano in Nigeria and Bamako in Mali, over a 30-year period (1992–2022). By employing various base temperatures (22 °C to 30 °C), the research revealed divergent patterns between the two cities, with Kano showing an upward trend in CDDs, indicating increasing cooling energy demands, while Bamako demonstrated a slight decrease in CDD over the same period. The analysis identified significant peaks in cooling demands during specific years, notably 1998 and 2015, which coincided with global warming intensification and climatic anomalies like El Niño [62] events. While the research provides valuable insights for local energy planning and policy development, its geographical scope, limited to just two cities, may not fully capture the diverse climatic conditions corresponding energy requirements across the West African region.

In this regard, the current study addresses critical gaps in climate-energy research by pioneering the first comprehensive integration of climate classification and building energy demand mapping across North Africa. While previous studies have focused on isolated regions, our study aims to develop a more comprehensive spatial mapping of heating and cooling degree days specifically for North Africa, addressing the notable research gap in this region where studies have primarily localized (e.g., Algeria, Morocco) rather than regional in scope. This research creates the first cohesive cross-border analysis of climate-driven building energy demands in this climate-vulnerable region.

3. Methodology

The research methodology is quantitative, similar to previous studies [48,63], and comprises three main stages. Fig. 1 illustrates the study's conceptual framework. First, the data acquisition was done via the NASA/POWER (Prediction of Worldwide Energy Resources) database [64] which is widely used as a platform for many climatic parameters over different periods: daily, monthly and yearly during long time periods. In this case, the collected climate parameters cover temperatures (maximums T_max) and minimus (T_min), relative humidity rates (RH_max, RH_min), rainfall, and wind speed. Secondly, the heating degree days (HDD) and cooling degree days (CDD) were calculated based on ANSI/ASHRAE 169–2020 [65,66]. Finally, the calculated heating and cooling degree days allowed us to map new climate zones in North African countries and develop a set of refined recommendations to be integrated into the regulation of each country and much globally in the MENA region through the building energy balance.

3.1. Overview of current climate zoning of the study area

Six North African geographic territories were selected, namely Egypt, Libya, Tunisia, Algeria, Morocco, and Western Sahara. The study scope covered 108 weather stations in total, implemented over the selected territories (Fig. 2). Furthermore, these weather stations are distributed differently within various zones as follow: 41 stations in Algeria, 12 stations in Morocco, 20 stations in Egypt, 16 stations in

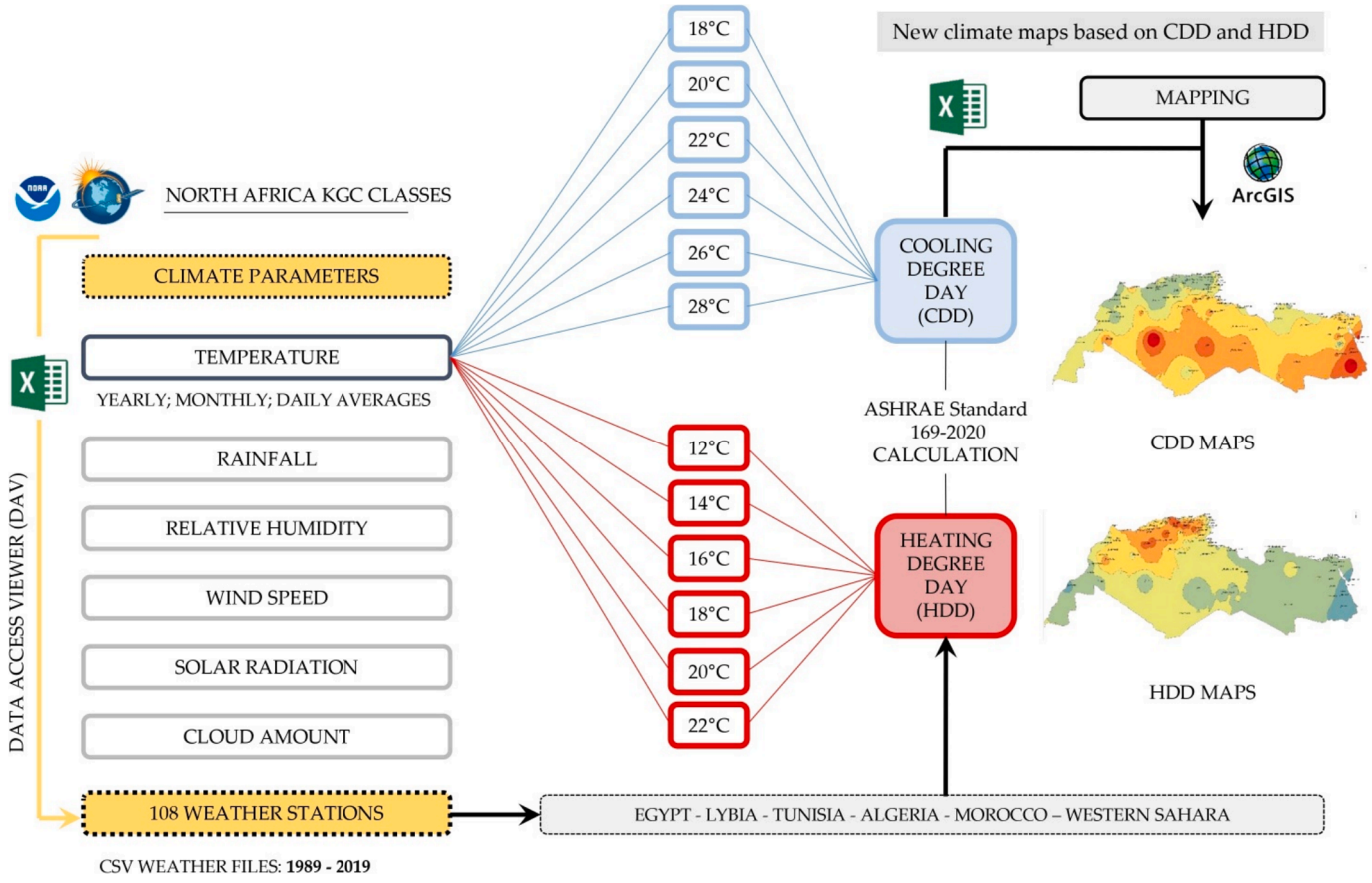

Fig. 1. Study conceptual framework and methodological research approach.

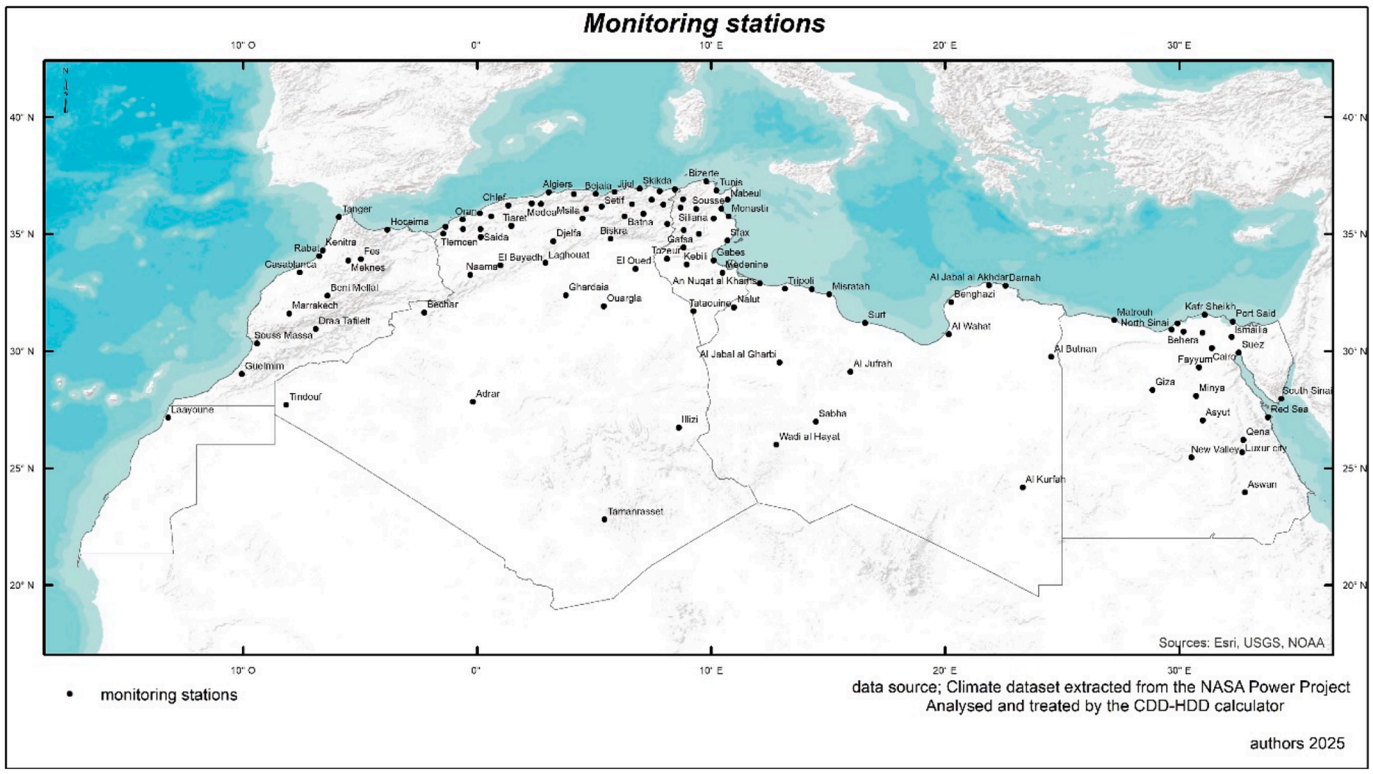

Fig. 2. Geographical distribution of weather stations across the entire study area.

Libya, 18 stations in Tunisia, 01 station in Western Sahara. All stations' locations and references were taken from the NOAA repository 'climate one building' [67]. It should be noted that the current study kept one single official station from each selected zone, and this one contains up to one station within it.

According to the building thermal regulations of each territory, several distinctions of climatic zones are linked to building energy use. Starting from Algeria, where the local thermal regulations (DTR C3-3) [60] identify six distinct zones: zone (A) covers the North of the country including the coastal ribbon; (B) situated at the southern frontier of the zone (A); zone (C) situated in the south part of the zone (B), including the highlands; zone (D) covers the South of Algeria with its large desert; (B) and (D) representing subzones within (B) and (D) zones respectively. Furthermore, in Tunisia, there are three different zones [68]: (ZT1) covers coastal zones; (ZT2) includes the Northern upland plateau; and zone (ZT3) includes the Southern upland plateau. In Egypt, the Housing and Building National Research Centre (HBRC) divides the country into eight climatic zones [69]: (1) North coast region; (2) Delta and Cairo region; (3) Region of Northern upper Egypt; (4) Region of Southern upper Egypt; (5) East coast region; (6) Altiplano region; (7) Desert region; and (8) Region of Southern Egypt. Moreover, the Regulatory Thermal Code in Morocco (RTCM) divides the country into six different zones [70]: (1) polarized by Agadir city; zone (2) polarized by Tangier city; zone (3) polarized by Fes city; zone (4) polarized by Ifran city; zone (5) polarized by Marrakech city; and zone (6) polarized by Al-Rachidia city. Unlike other countries, Libya doesn't have a specific thermal regulation guideline for buildings, where climate zones remain general and directly related to its own geography: (1) Coastal region, (2) Mountains region, and (3) Desert region.

On the other hand, North Africa has varied population densities, distributed within different regions from coastal cities to continental lands and desert territories (Fig. 3). Consequently, the population density decreases gradually from north and coast toward internal lands and desert areas and vice versa due to various government policies and tertiary and socio-economic criteria of local strategies. The population density balanced from less than 1,00,000 inhabitants to up than 2,000,000 inhabitants [71]. Egypt as one of the densely populated countries of Africa has the highest population rate. Cairo counts 22.6 million in the greater metropolitan area in 2024. Rabat, Algiers, Tunis, Tripoli capitals have population densities of 1.9 million, 3.3 million, 2.5 million, and 1.19 million, respectively in 2024 [71].

3.2. Heating and cooling degree days calculation

The study is based on the NASA/POWER database [72,73,74] for climate data collection within a time collapse from 1989 to 2019. In fact, the NASA/POWER project was initiated in 2003 to provide daily solar and meteorological datasets to support renewable energy, sustainable buildings and agroclimatology at 1°x1° geographic coordinate grid, with free access to solar radiation data, meteorological data, and many other related information for geographical locations around the globe. Additionally, many studies have reported the high accuracy and feasibility of the NASA/POWER database for architecture, urban planning and agronomic research throughout different worldwide continents, in South America, Europe, Africa, and Australia [72,73,75].

The NASA/POWER has a nested approach for temporal data processing. The POWER uses a set processing hierarchy for stored data values when this operation records 24-hour values and provides a daily max, min or average (mean of hours). This process allows to carry out the monthly averages (mean of the days), annual averages (mean of the months), and climatology averages (mean of the annuals). It should be noted that the current study is primarily based on temperatures recorded at two-meter levels (T2M_MAX), (T2M_MIN) and (T2M_AVG) as the main parameters to calculate HDD and CDD. Additional meteorological parameters were relative humidity, wind speed, and rainfall. All these parameters remain to the Sustainable Buildings (SB) community, providing hourly and daily time series formats, as well as climatologically, monthly and annual average values.

On the other hand, these weather files have been downloaded in CSV formats, whereas the geographic coordinates of the weather stations

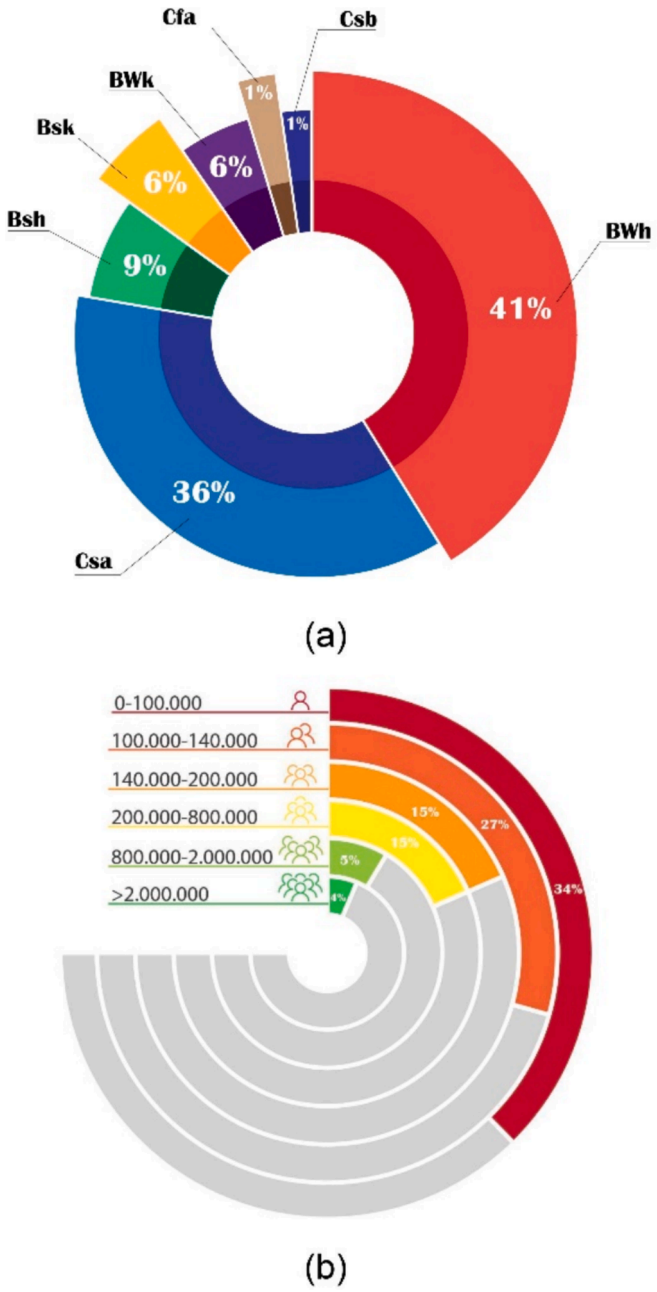

Fig. 3. Climate zones distribution and population demographics across North African regions: (a) Percentage distribution of distinct climate zones in North Africa; (b) Population distribution within North African urban areas.

were recovered from the NOAA repository for climate data. This later encompasses worldwide regions, in TMY files, into different formats such as EPW and DDY, including the studied zone North Africa 'Africa-Region 1' [67]. All the weather stations have an official WMO reference number known as matriculation.

The calculation of the Heating Degree Days (HDDs) and Cooling Degree Days (CDDs) for each city is mainly based on their daily mean temperatures. Degree day values are essential data for one who needs to manage the significant energy consumption related to the heating or cooling of buildings. Degree day value quantifies how cold or hot the weather has been as a single index number for a particular region and a particular period like a month or week, which allows proper accounting for the effect of weather conditions on energy consumption. In this regard, HDDs and CDDs are widely used indicators to examine cold or warming and quantify the heating and cooling demand. HDDs are defined as the deviation of the mean daily temperature from a heating base temperature of 18.3 °C [76,77]. The heating degree days' values have been calculated using the following equations [41,70]:

$$\mathrm{HDDdaily} = (\mathrm{Tb} - \mathrm{Ta}) + \tag{1}$$

$$HDDmonthly = \sum_{i=1}^{m} HDDdaily, i \tag{2}$$

$$HDDyearly = \sum_{j=1}^{12} HDDmonthly, j \tag{3}$$

$$HDDyearlyaverage = \frac{\sum_{k=1}^{30} HDDyearly}{30} \tag{4}$$

In the equations, Ta (°C) is the daily mean ambient temperature, Tb (°C) is the base point temperature, and HDD is the heating degree day number. The positive sign in Equation (1) shows that only the positive values of temperature difference (Tb − Ta) should be considered for HDD. If this temperature difference is negative, it should be considered as zero [76]. The annual HDDs of 108 selected cities have been calculated in comparison to six different base temperatures: 12 °C, 14 °C, 16 °C, 18 °C, 20 °C and 22 °C.

On the other hand, CDDs measure how warm a given location is, by comparing the mean outdoor temperatures recorded daily with a base temperature (usually 65 °F or 18 °C) [78]. Daily, monthly, yearly and yearly average heating degree day numbers for each city have been calculated using Equations (5) to (8) [48,77]:

$$\mathrm{CDDdaily} = (\mathrm{Ta} - \mathrm{Tb}) + \tag{5}$$

$$CDDmonthly = \sum_{i=1}^{m} CDDdaily, i \tag{6}$$

$$CDDyearly = \sum_{j=1}^{12} CDDmonthly, j \tag{7}$$

$$CDDyearlyaverage = \frac{\sum_{k=1}^{30} CDDyearly}{30} \tag{8}$$

Using the same method as HDD, the positive sign in Equation (5) shows that only the positive values of temperature difference (Ta − Tb) should be considered. If this temperature difference is negative, it should be considered as zero. The annual HDDs of 108 selected cities have been calculated in comparison to six different base temperatures: 18 °C, 20 °C, 22 °C, 24 °C, 26 °C and 28 °C.

It should be noted that the selection of the base temperatures for HDDs and CDDs calculations is primarily related to the regional climate diversity, as North Africa encompasses diverse climate zones ranging from Mediterranean coastal areas to arid desert regions. Moreover, the selection also accounts for building stock variation, which differs significantly in terms of construction materials, insulation standards, and architectural design covering both traditional buildings and modern ones with mechanical cooling and heating systems.

3.3. Spatial mapping of heating and cooling degree days

The visualization of the spatial distribution of HDDs and CDDs results was designed using a geographic information system (GIS) technique [47,79,80]. GIS tools are commonly used to illustrate the spatial data and visualization issues associated with multiscale geographic data. GIS tools allow direct viewing of the spatial difference, and a direct comparison of values associated with the region's use pattern on the map. To visualize the spatial distribution of HDDs and CDDs values over 30 years, it was necessary to use specific spatial interpolation techniques [77,81].

To overcome this limitation, spatial interpolation techniques are

used. These methods allow for estimating HDD and CDD values between known measurement points.

Moreover, kriging is a particularly effective spatial interpolation method available in ArcGIS software [82,83]. It takes into account the spatial structure of the data to create continuous and accurate maps of HDDs and CDDs. The resulting maps can be used for urban planning, energy resource management, and the development of climate change adaptation policies. This approach provides a deep understanding of climate variations and their energy implications, allowing for better management and planning of resources at regional or national scales.

The spatial delimitation of climate zones in North Africa is based on the analysis of variations in HDDs and CDDs over 30 years, from 1989 to 2019. As mentioned previously, the current study utilized data provided by the DATA POWER ACCESS VIEWER platform, which is a free online tool developed by NASA that provides access to meteorological and climate data. The GIS modeling sampling comprises 108 measurement stations distributed across the entire study area in North Africa.

In this work, data processing was mainly carried-out using ArcGIS 10.8 software [84]. This Geographic Information System (GIS) offers a wide range of spatial interpolation methods [79], which allows for exploring different approaches to accurately determining energy needs.

This approach allowed to obtain a detailed spatial representation of the energy needs related to temperature impact in the region. The research highlighted the climatic disparities between the various regions of North Africa, thus identifying areas with high demand for heating or cooling. By using ArcGIS interpolation techniques, we transformed these point data into continuous maps, providing a detailed spatial representation of climatic variations across the region.

Accordingly, our study aimed to map the distribution of Heating Degree Days (HDD) and Cooling Degree Days (CDD) across the study area. To achieve this objective, we implemented the following workflow (Fig. 4) to analyze and map the spatial distribution of HDDs and CDDs in the investigated region:

4. Results

4.1. Spatial distribution of HDDs and CDDs across the studied locations

Annual average HDDs and CDDs of 108 cities located in different regions within North African territories, Egypt, Libya, Tunisia, Algeria, Morocco and Western Sahara, have been calculated using equations (1) to (8), based on the daily average temperature data of each city obtained from the NASA/POWER database over 30 years. As reported previously, the annual HDD quantities have been calculated for six different temperatures: 12 °C, 14 °C, 16 °C, 18 °C, 20 °C and 22 °C. Across North Africa, at different base temperatures, the highest calculated numbers of HDDs were: 816, 1145, 1529, 1953, 2421, and 2932, consistently achieved in the city of Bordj Bou Arreridj (604440) at an altitude of 957 m, in the 'High Plateaus' region in central Algeria. The elevation of altitude was a crucial factor influencing the increase in HDD numbers compared to lower-altitude coastal cities, but it was not the sole factor. Consequently, the highest altitudes across the countries showed particularly high values: Draa Tafilelt (Morocco), Kessrine (Tunisia) which presented the highest altitude in their respective territories, followed by Al Jabal

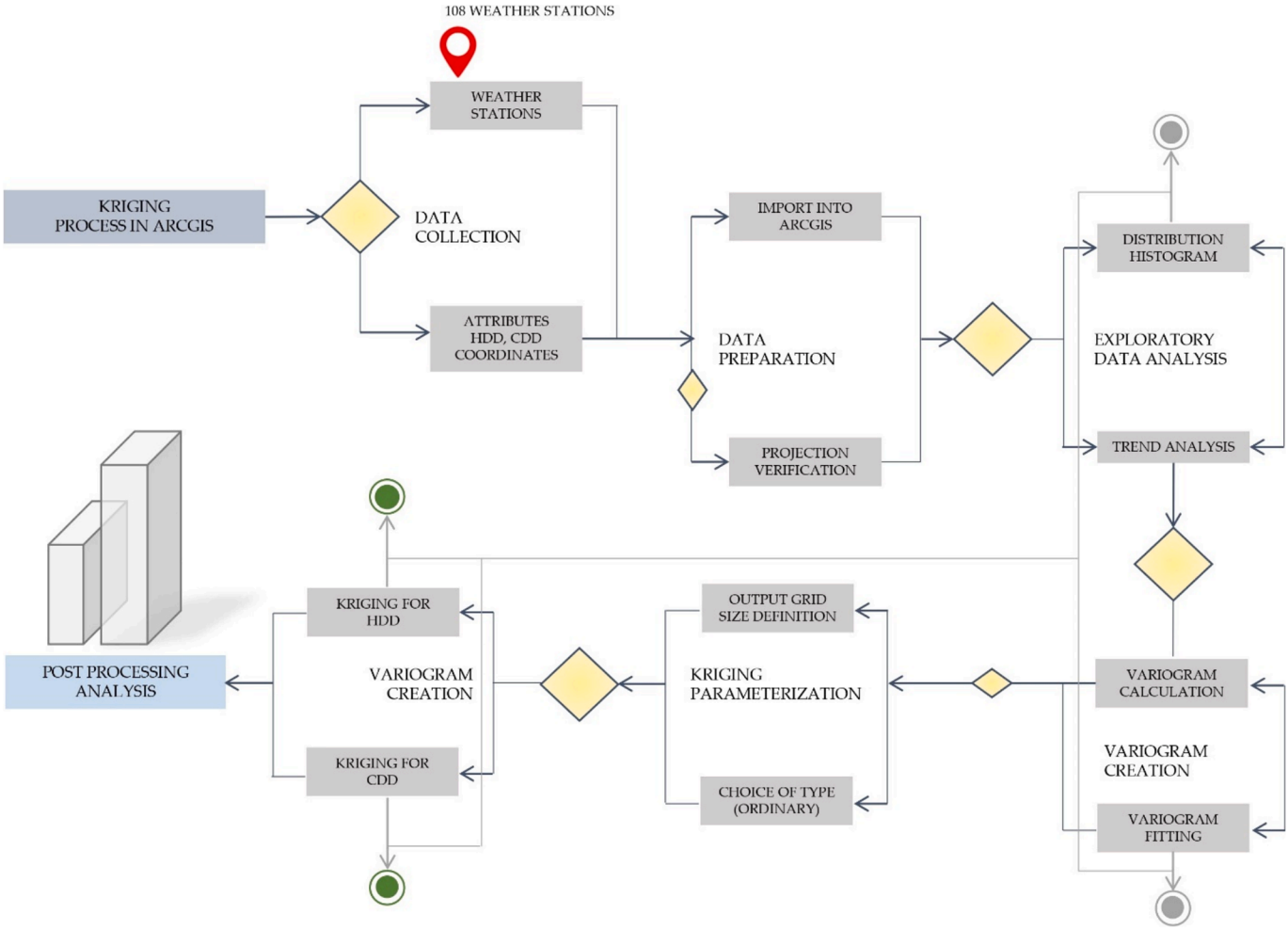

Fig. 4. The developed workflow of HDDs and CDDs analysis and mapping via ArcGIS model.

Al Akhdar (Libya), Giza (Egypt), with HDDs numbers of 1418, 1436, 417, 587, on altitudes 1153.1 m, 707 m, 648 m, and 130 m, respectively at a base temperature of 18 °C. Comparatively, the BSk climate zone represented the highest heated demand among different zones, while the BWh zone acquired the lowest HDD values. For instance, two other factors can significantly influence heating demands: geographical proximity to the Mediterranean or Atlantic coasts, and population demography, with populated areas like Giza in Egypt.

As shown in Fig. 5, the spatial distribution of the annual HDDs varied from one geographic zone to another, with notably high values in specific locations. Before analyzing, Fig. 5 displays specific concentrations of HDDs, which are > 500 at the calculated six base temperatures. Consequently, these geographical areas are concentrated in zones where generally located on Latitudes above 32° and longitudes between −1° and 10°, regardless of their climate zones. Furthermore, from the 14 °C base temperature upward, these areas include additional zones located at the same latitudinal coordinates but with longitudes between 25° to 34 °C. On the other hand, the most commonly observed ranges of annual HDDs averages were: 1 < HDDs < 250 at 12 °C, 1 < HDDs < 450 at 14 °C, 1 < HDDs < 650 at 16 °C, 100 < HDDs < 1000 at 18 °C, 200 <

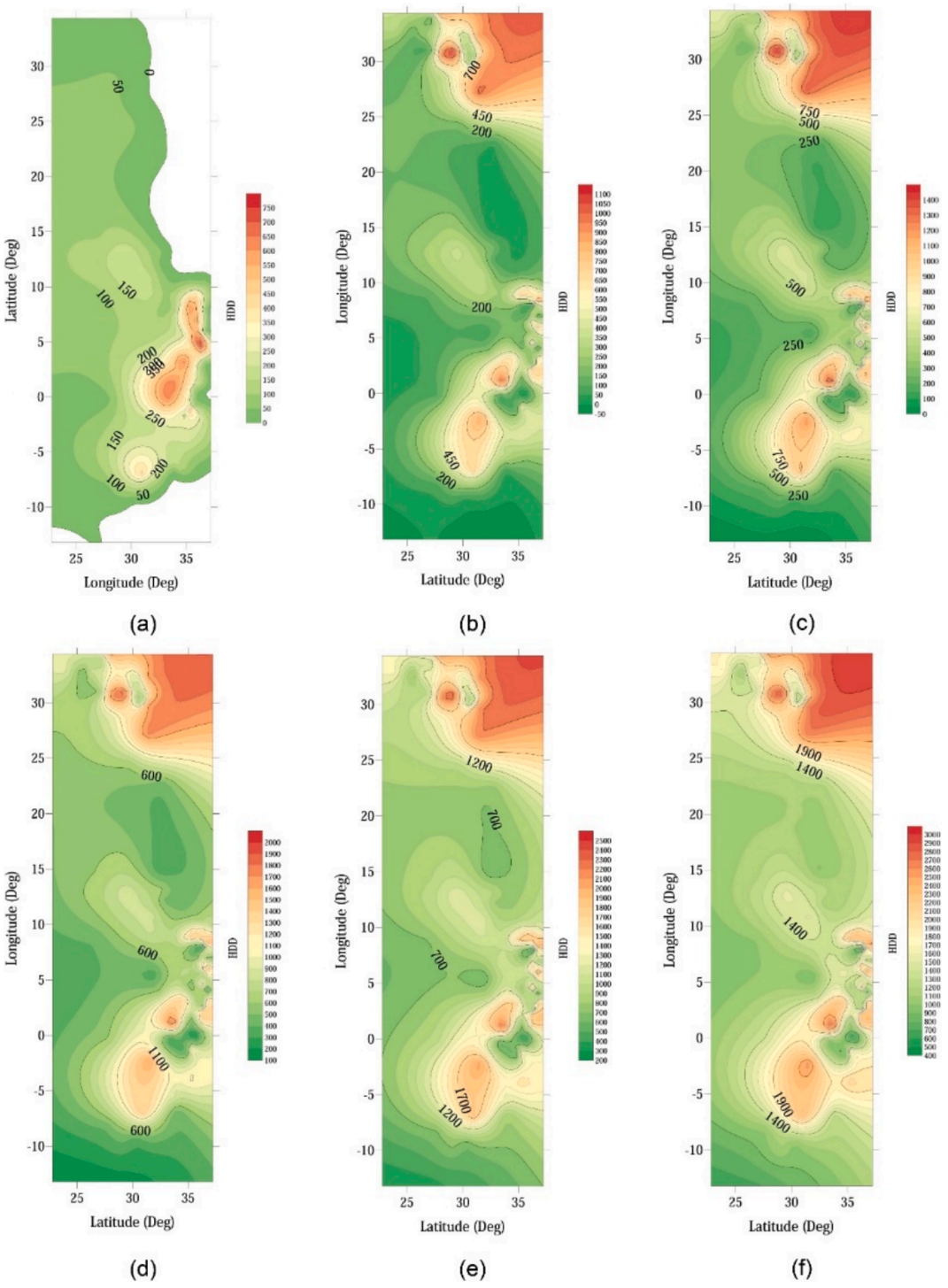

Fig. 5. Spatiotemporal distribution of HDDs number within the investigated stations over 30-year with different base temperatures: (a) 12 °C; (b) 14 °C; (c) 16 °C; (d) 18 °C; (e) 20 °C; and (f) 22 °C.

HDDs < 1200 at 20 °C, and 400 < HDDs < 1600 at 22 °C. These ranges were mostly distributed throughout the North African lands.

Using the same methodology approach as for HDDs, CDDs quantities were calculated for the same 108 cities for six different base temperatures, 18 °C, 20 °C, 22 °C, 24 °C, 26 °C, and 28 °C. As observed from the CDDs calculations, the high values were obtained consistently throughout the city of Adrar (606200) at an altitude of 280 m, in the Southern desert of Algeria with: 3169, 2658, 2190, 1764, 1381, and 1041, respectively at the six different base temperatures. Notably, the BWh climate zone was the highest cooling demand zone, regardless the altitude of locations. Particularly, some cities located in the BWh climate zone revealed very low CDDs quantities: Laayoune in Western Sahara (altitude of 199 m); Port Said (6 m) and Matruh (28.7 m) in Egypt. Other cities in the same climate zone were meanly low compared to BWh areas. On other hand, The Csa climate zone showed the lower CDDs quantities, more specifically inside the coastal cities within the studied countries. In this regard, the lowest CDDs annual averages were obtained in the city of Kenitra (Morocco) located at an altitude of 6 m with 676, 335, 104, 18, 3, and 1, respectively at the base temperatures. With sea breeze, proximity to the coast is considered a main factor for

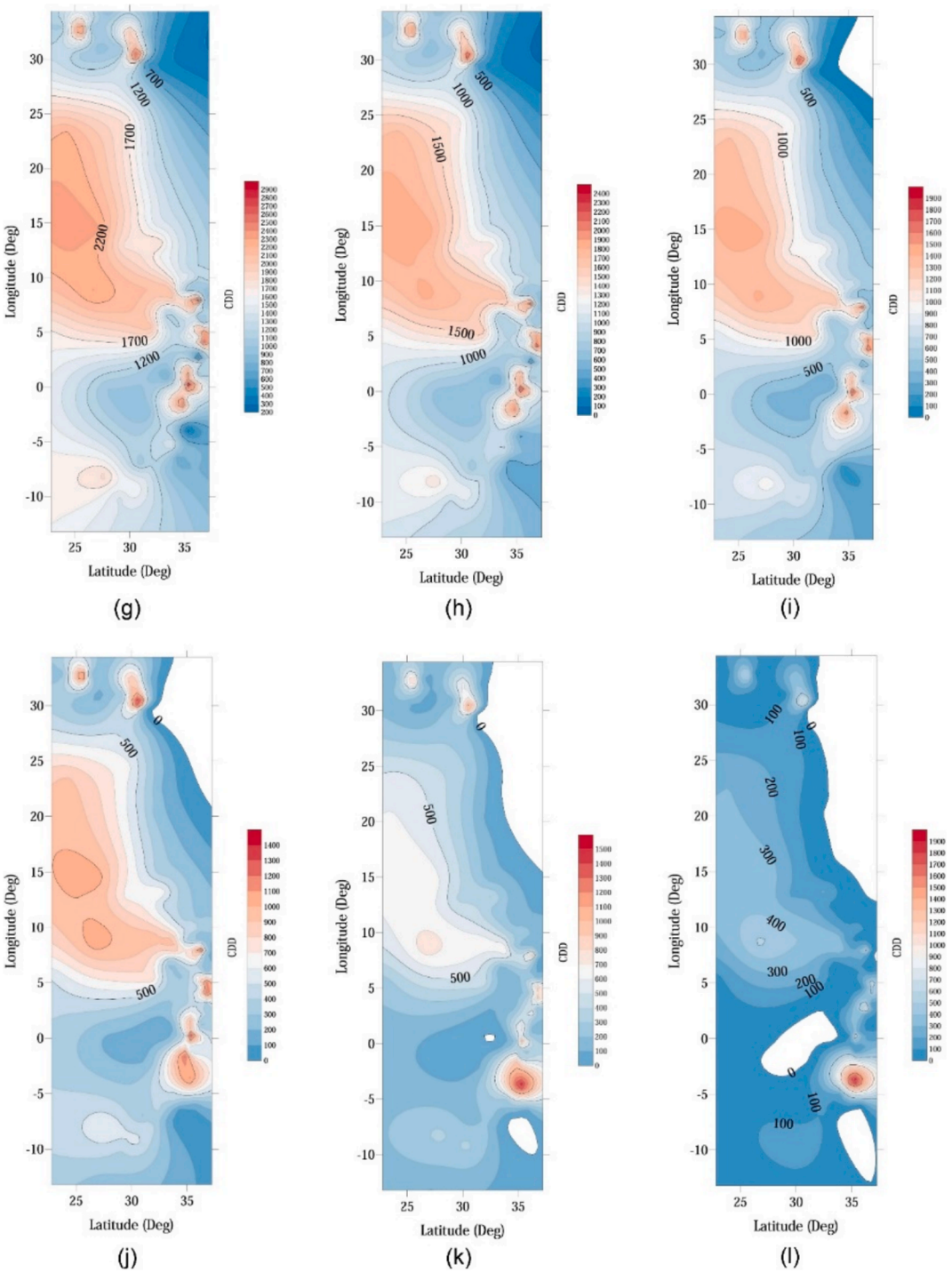

Fig. 6. Spatiotemporal distribution of CDDs number within the investigated stations over 30-year with different base temperatures: (g) 18 °C; (h) 20 °C; (i) 22 °C; (j) 24 °C; (k) 26 °C; and (l) 28 °C.

controlling cooling demands, where continental regions require much more cooling compared to coastal regions throughout North Africa.

As shown in Fig. 6, the spatial distribution of the calculated CDD quantities varied from one geographic area to another by the six different base temperatures. The highest cooling demand concentration ranges > 1600 was located on latitudes between 27° and 30° with longitudes between 0° and − 5°, particularly in the BWh climate zone. On the other hand, the large commonly observed ranges of annual CDDs averages were: 200 < CDDs < 1600 at 18 °C, 1 < CDDs < 1200 at 20 °C, 1 < CDDs < 900 at 22 °C, 100 < CDDs < 1000 at 24 °C, 1 < CDDs < 600 at 26 °C, and 1 < CDDs < 800 at 28 °C. These ranges cover most of the North African lands.

4.2. Analysis of differences in HDD and CDD quantities among the investigated territories

The calculation results of HDD and CDD quantities for each geographic territory are reported as box plots in Fig. 7. Starting with Algeria, across all the meteorological stations the country exhibited a gradual increase on HDDs values' medians with: 219, 412, 694, 1052, 1466 and 1934 at 12 °C, 14 °C, 16 °C, 18 °C, 20 °C, and 22 °C, respectively. Consequently, the differences accumulated interquartile (Q3) and (Q1) $\Delta_{Q3.Q1\_Algeria\_HDD}$ were: 393, 545, 659, 750, 908 and 1013, respectively at the same base temperatures. On the other hand, Egypt as biggest populated country in North Africa, revealed in contrast low HDD medians compared to Algeria with: 14, 61, 164, 339, 575, and 915 at the base temperatures. Furthermore, the differences interquartile obtained $\Delta_{Q3.Q1\_Egypt\_HDD}$ were: 21, 71, 132, 160, 185, and 223. In this regard, results indicate a significant difference between the two countries in their heating cooling demands.

Otherwise, regarding the annual CDD averages, Algeria exhibited a decrease compared to its HDD averages. CDD medians were varied between 1070, 765, 511, 307, 152 and 56 at 18 °C, 20 °C, 22 °C, 24 °C, 26 °C, and 28 °C, respectively as base temperatures. Thus, the differences regarding the quartiles $\Delta_{Q3.Q1\_Algeria\_CDD}$ were 416, 297, 288, 247, 187, and 109, respectively, at the same base temperatures.

In Eastern North Africa, Egypt revealed an elevation in the annual CDD averages compared to HDDs, which clearly reflects the high demand for cooling systems. Consequently, CDD medians varied between 1910, 1445, 1034, 681, 433, 193, respectively at the base temperatures. Further, differences interquartile $\Delta_{Q3.Q1\_Egypt\_CDD}$ were 740, 677, 617, 546, 454, and 443, respectively at the same base temperatures. Accordingly, results reflect the high cooling demand in Egypt compared to Algeria, regardless of the nearby climate conditions in various

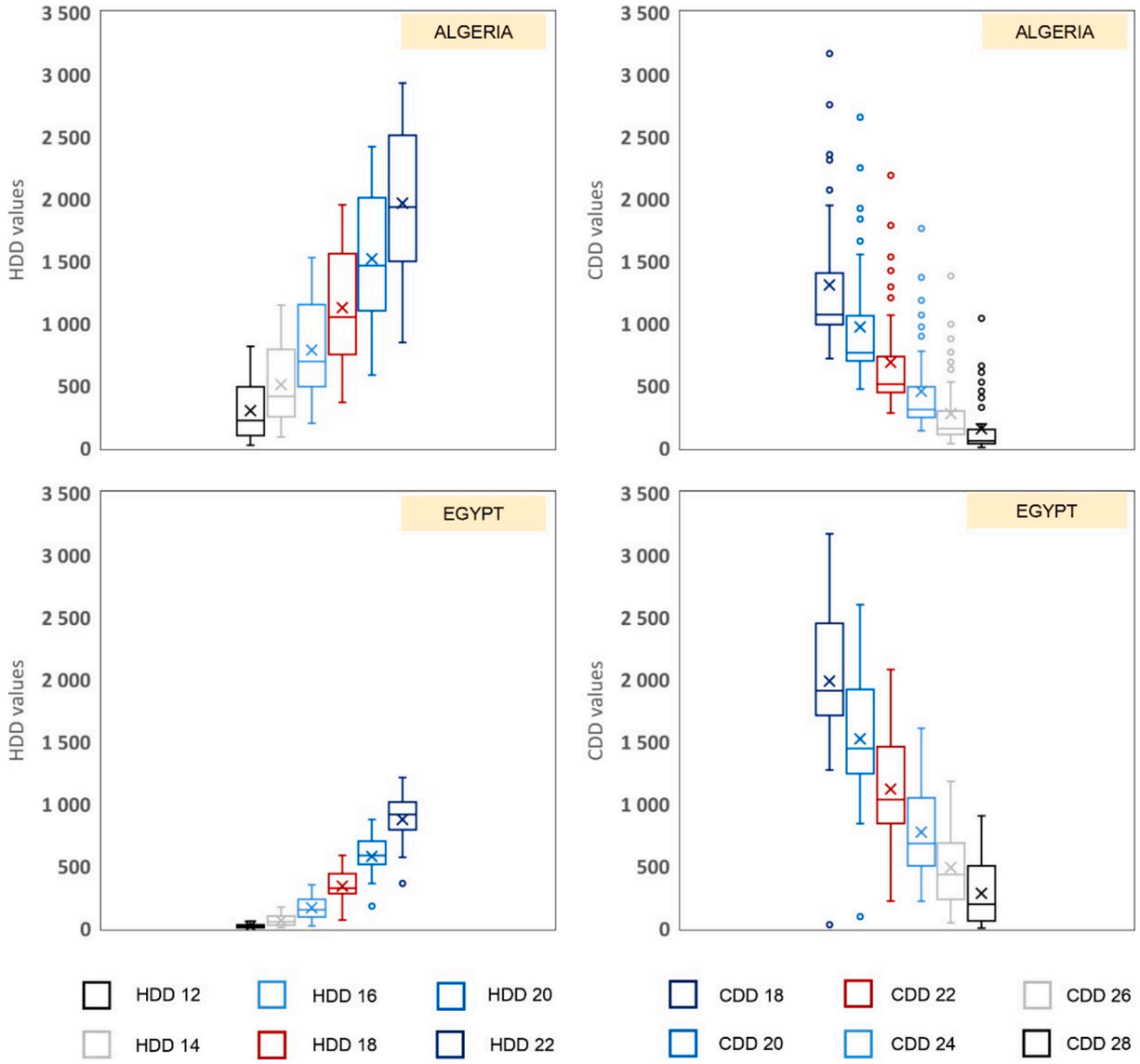

Fig. 7. Box plots analysis of the HDDs and CDDs variations in Algeria and Egypt **over 30 years**.

geographical areas.

Fig. 8 shows the HDDs and CDDs annual averages in Libya and Tunisia. Across all the meteorological stations in Libya, a slight gradual increase regarding the HDDs quantities, while the medians varied between: 39, 130, 288, 512, 793, and 1150, respectively at the reported base temperatures, that is slightly higher to Egypt as an eastern neighbor. Furthermore, the differences interquartile of Libya $\Delta_{Q3.Q1\_Libya\_HDD}$ were 80, 163, 207, 243, 197, and 156, respectively at the base temperatures. Otherwise, Tunisia as a western neighbor to Libya, revealed high HDDs annual averages as Libya's heating demands, whereas the medians were: 161, 252, 458, 764, 1133 and 1540, respectively at the base temperatures. Moreover, the interquartile differences $\Delta_{Q3.Q1\_Tunisia\_HDD}$ varied between: 190, 274, 328, 378, 428, and 483, respectively. Despite the low land area of Tunisia, it shows high heating demand quantities compared to Libya and specifically to Egypt, which is bigger and populated.

On the other hand, the CDDs annual averages in Libya showed an elevation compared to its HDDs quantities. The calculated medians varied between: 1712, 1281, 885, 559, 224, and 116 at 18 °C, 20 °C, 22 °C, 24 °C, 26 °C and 28 °C as base temperatures. Consequently, their interquartile differences $\Delta_{Q3.Q1\_Libya\_CDD}$ were 456, 446, 412, 360, 289, and 189, respectively at the same base temperatures. Otherwise, Tunisia exhibited a slight decrease in CDDs annual averages compared to HDDs, lower cooling demand than Libya and Egypt and higher than Algeria. The medians were: 1311, 940, 623, 367, 182, and 80, respectively at the base temperatures. Thus, the interquartile differences $\Delta_{Q3.Q1\_Tunisia\_CDD}$ were among 470, 402, 333, 271, 198, and 86, respectively, at the base temperatures.

Fig. 9 shows the annual averages of HDDs and CDDs in Morocco and Western Sahara at various base temperatures. For HDD numbers, the results reveal a slight gradual increase in heating demands across all base temperatures. The medians varied between 125, 242, 437, 809, 1182, and 1615 at the base temperatures of 12 °C, 14 °C, 16 °C, 18 °C, 20 °C, and 22 °C, respectively. The interquartile differences $\Delta_{Q3.Q1\_Morocco\ \&\ WS\_HDD}$ also show an increase across the same thresholds.

On the other hand, CDD values in Morocco and the Western Sahara, as shown in the right panel, indicate an elevation in cooling demands compared to HDD values. The medians varied between 1246, 922, 628, 370, 276, and 128 at base temperatures of 18 °C, 20 °C, 22 °C, 24 °C, 26 °C, and 28 °C, respectively. This demonstrates a sharp decrease in cooling demand as the base temperature increases. The interquartile differences $\Delta_{Q3.Q1\_Morocco\ \&\ WS\_CDD}$ followed a similar trend, declining from 456 to 189 across the thresholds.

The decadal analysis of HDDs and CDDs quantities across the study area from 1989 to 2019 revealed significant climatic shifts and energy demand patterns (Fig. 10 and Appendix A).

Algeria showed a coastal-desert distinction. Coastal cities like Algiers experienced moderate heating needs, with HDDs at 12 °C base temperature peaking at 31.6 in 1999–2008, while desert regions like Adrar recorded minimal HDDs values (2000 at 28 °C), although these regions experienced moderate increases in CDDs. With 80 % of Algeria's population concentrated along the northern regions, these areas particularly

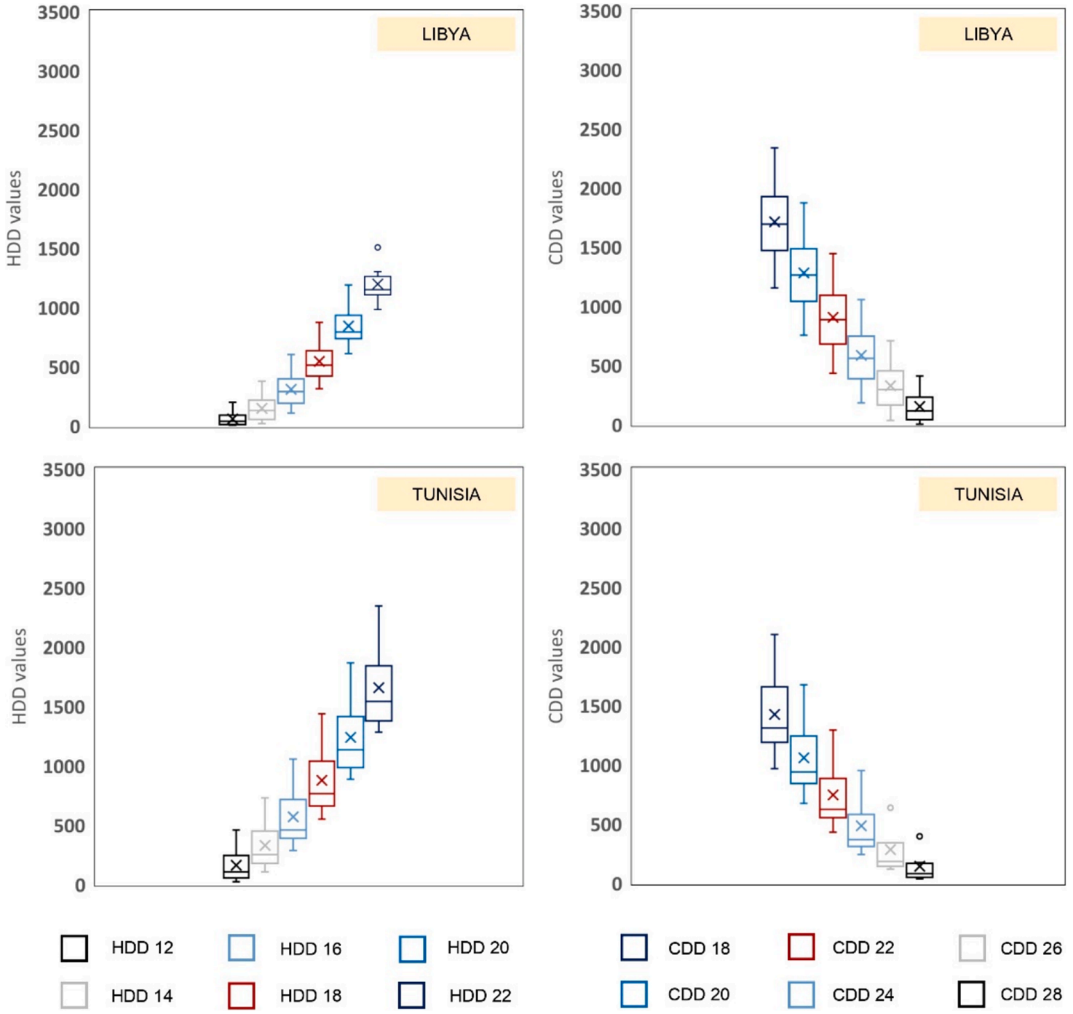

Fig. 8. Box plots analysis of the HDDs and CDDs variations in Libya and Tunisia **over 30 years**.

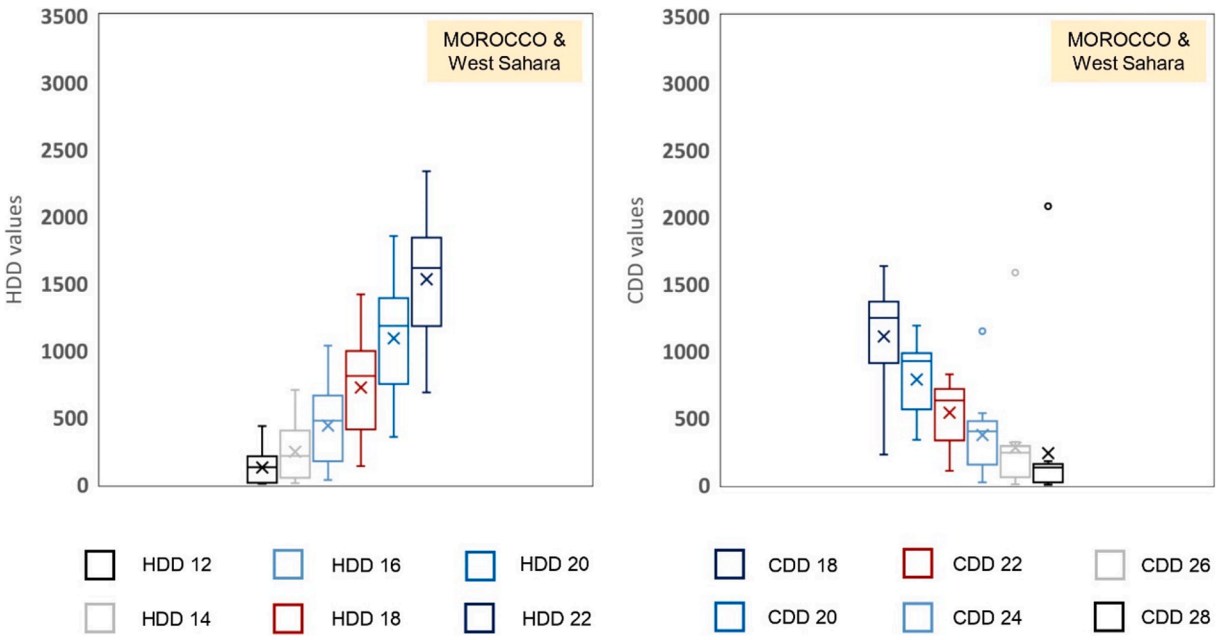

Fig. 9. Box plots analysis of the HDDs and CDDs variations in Morocco and Western Sahara **over 30 years**.

facing significant vulnerability to energy consumption resulting from cooling system needs.

Western Sahara, as an arid land, recorded near-zero HDDs in Laayoune region with 2.4 at 12 °C, versus extreme CDDs quantities. The CDDs at 28 °C increased by + 63.9 over three decades.

Tunisia reflected a balance of Mediterranean and desert influences. Northern cities like Kef had moderate HDDs (112.7 at 12 °C in 1989–1998) and constant CDDs, while southern desert regions like Gabes showed CDDs at 18 °C increased from 633.6 to 639.4.

In Morocco, mountainous zones like Beni Mellal had persistent HDDs quantities (236.0 at 12 °C in 1989–1998), while coastal cities like Casablanca presented CDDs at 18 °C increased from 902.9 to 991.4.

Egypt exhibited a distinct climatic profile characterized by minimal heating demands and significant cooling requirements. Thus, HDDs were consistently low across decades, with cities like Aswan recording HDDs values below 11 at 12 °C. Conversely, CDDs had substantially increased, driven by elevated temperatures and accelerated urbanization. For instance, Aswan's CDDs at 28 °C increased from 658.6 in 1989–1998 to 861.3 in 2009–2019. Additionally, coastal regions like Alexandria also showed notable increases in CDDs, highlighting the growing demand for cooling infrastructure across urban and rural areas.

Libya's climatic trends over three decades revealed increasing cooling demands and moderate heating requirements. Accordingly, coastal cities like Benghazi showed declining HDDs, dropping from 3.7 at 12 °C in 1989–1998 to 3.0 in 2009–2019, reflecting moderate winters' periods. Furthermore, CDDs had risen significantly, with Benghazi's CDDs at 18 °C increased from 1255.1 to 1369.9 over the same period. Moreover, desert areas such as Al Kufrah revealed extreme CDDs values exceeding 2000 at 28 °C base temperature. Coastal cities also exhibited a CDD increases, influenced by urbanization and Mediterranean warming trends. Overall, Libya's energy demand is increasingly dominated by cooling requirements.

Consequently, comparative analysis reveals overall CDDs increases (15–40 %) across the region, with Egypt and Algeria experiencing the most remarkable rises. Coastal cities, influenced by humidity and population density, faced CDDs elevation with 3 to 5 times higher than desert regions in Sahara. Moreover, mountainous areas, such as in Morocco's Atlas, maintained constant HDDs and CDDs quantities. In fact, urbanization emerged as a critical factor: Algiers and Tripoli recorded CDDs rises between 20 and 30 % above rural averages.

Overall, energy implications are substantial. Cooling requirements constituted 70–90 % of total energy consumption in desert cities by 2019. Meanwhile, coastal regions experienced diminishing HDDs (e.g., Tunis with a 15 % reduction in HDDs at 12 °C), leading to reduced winter energy needs and allowing resources to be redirected toward cooling systems. However, fossil fuel dependency persists, with air conditioning accounting for 40–60 % of summer electricity demand in major cities such as Cairo and Marrakech.

Overall, Fig. 11 and Appendix B illustrate the spatial distribution of HDDs and CDDs across the entire studied region. Fig. 11, part (a), represents the initial Köppen-Geiger climate classification, compared to part (b) which shows the distribution of HDDs at a base temperature of 22 °C. Higher HDD values indicate greater heating demands, which are concentrated in the northern regions, with values ranging from 2400 to 2992. These areas reflect colder conditions and require more heating. Moving southward, HDD values gradually decrease, transitioning through moderate zones from 2000 to 2399 and 1200–1599, and eventually reaching low values of 381–399 in the central and southern areas. These regions experience warmer conditions with minimal heating requirements. The spatial trend follows a latitudinal gradient, with heating needs diminishing as temperatures increase toward the south.

Otherwise, Fig. 11, part (c), illustrates the spatial variation of CDDs at a base temperature of 18 °C. The highest CDD values, reflecting substantial cooling demand, are observed in the central and southeastern regions, where values range between 2400 and 3172. These areas correspond to hotter and arid climates with higher temperatures. Furthermore, surrounding zones with values of 2000–2399 and 1200–1599 indicate moderate cooling demands. On the other hand, the northern coastal areas exhibit the lowest CDD values of 676–799, where cooler temperatures reduce the need for cooling.

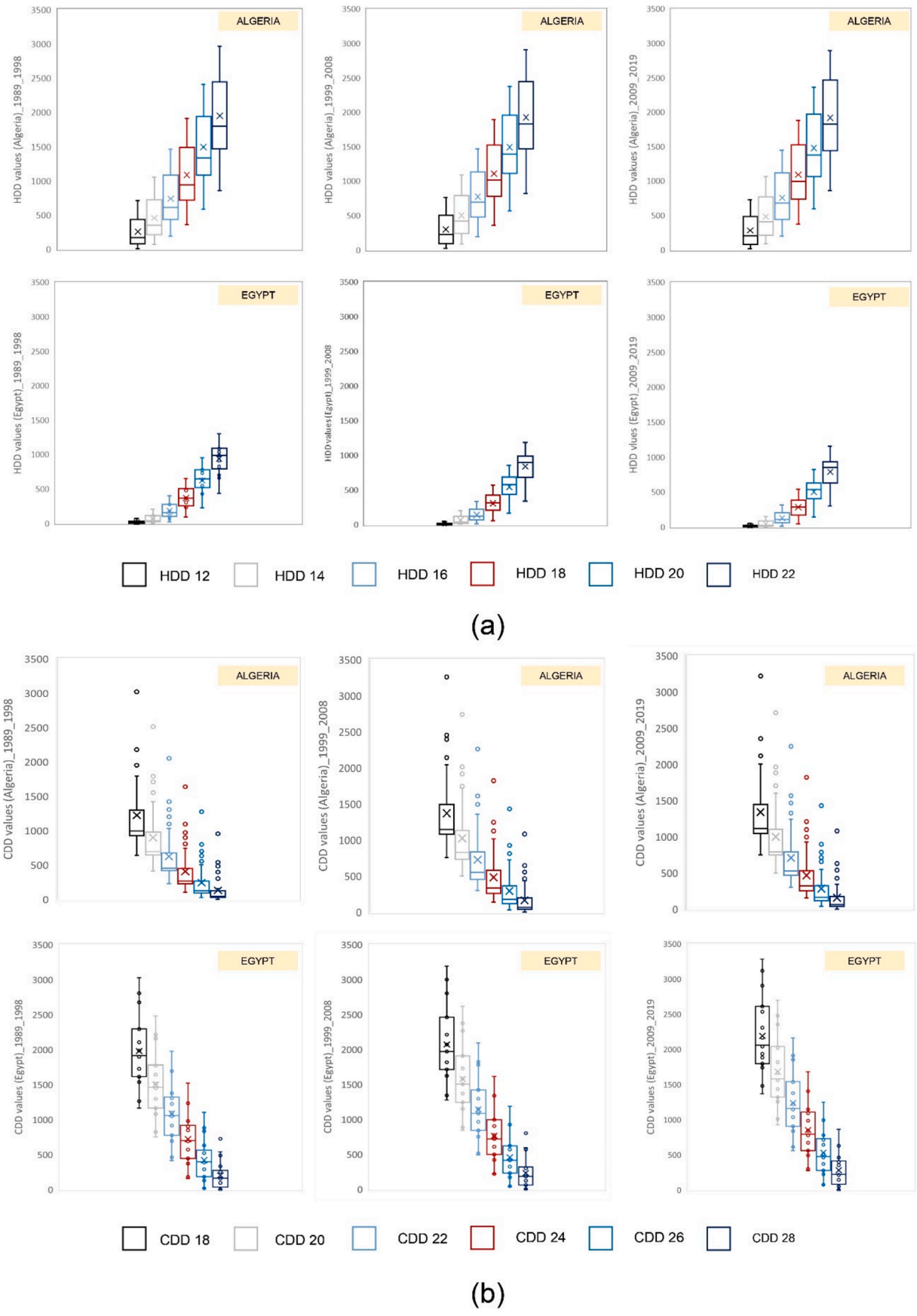

Fig. 10. Box plots of heating and cooling demands during three decades within the studied area: (a) comparative HDD quantities between Algeria and Egypt; (b) comparative CDD quantities between Algeria and Egypt.

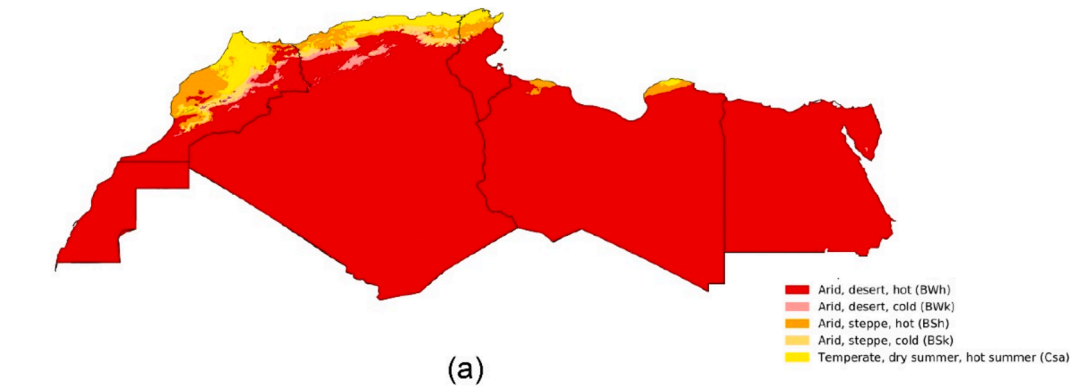

(a)

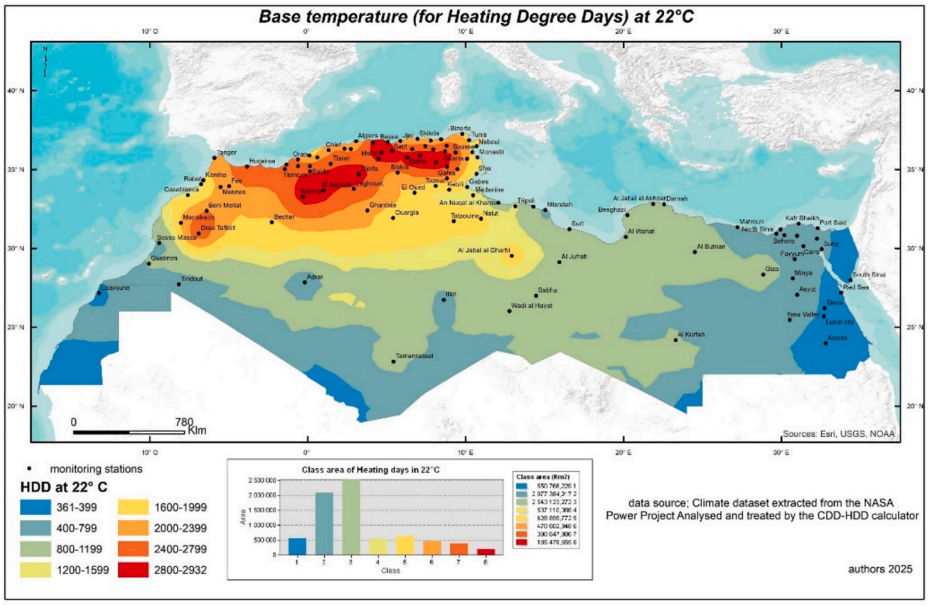

(b)

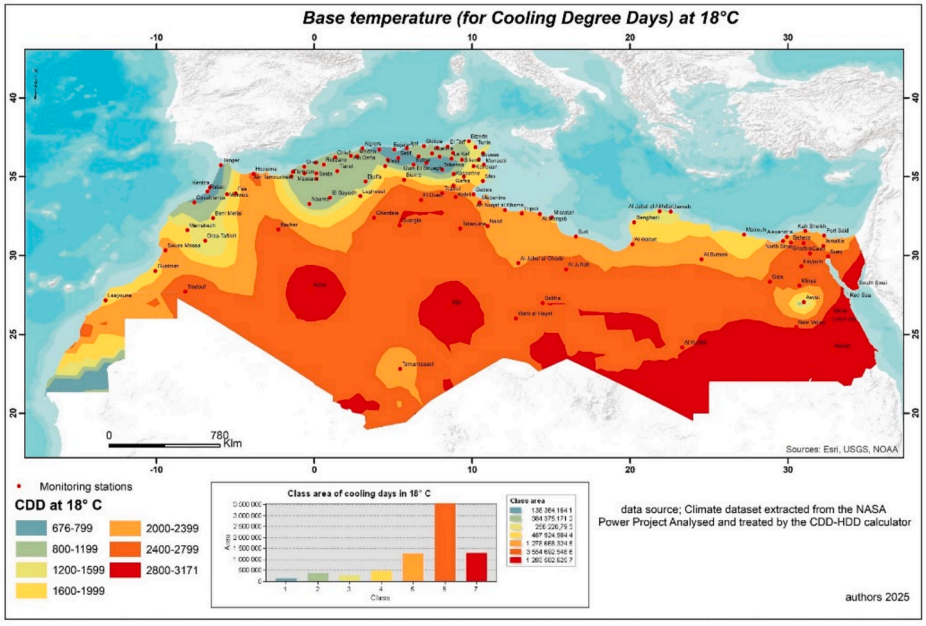

(c)

Fig. 11. Comparative map between current KGC, HDDs and CDDs maps within the investigated geographic territories in North Africa: (a) Köppen-Geiger climate classification (KGC) map; (b) HDD map at 22 °C base temperature; (b) CDD map at 18 °C base temperature.

5. Discussion

5.1. Summary and main findings

The study utilized meteorological data from 108 weather stations located across six North African geographic territories: Egypt, Libya, Tunisia, Algeria, Morocco, and Western Sahara. The analysis is based on a comprehensive and up-to-date dataset spanning 30 years (1989–2019), ensuring robust temporal and spatial coverage of climatic conditions.

A novel classification method for climate zones in North Africa was developed, achieving a spatial resolution of 3025 km^2, a significant improvement over the 12 321 km^2 resolution of traditional classifications. This increased granularity allows for detailed environmental characterization and provides deeper insights into the microclimatic variations across the region. The enhanced spatial precision facilitates a better understanding of the interplay between climatic factors and localized energy demands.

By employing Heating Degree Days (HDD) and Cooling Degree Days (CDD) as key metrics, the study refined the classification of existing Köppen-Geiger Climate (KGC) zones, including Csa, Csb, Cfa, BSh, BSk, BWk, and BWh. This approach enabled the identification of new sub-classifications within these zones, allowing for more accurate differentiation between regions previously grouped under similar climate categories (Appendix C). The incorporation of multiple base temperatures for HDD and CDD calculations further enhanced the accuracy of the climate zone delineations.

The analysis revealed that Algeria exhibits the highest climatic diversity in the region, encompassing up to seven distinct climate sub-classifications per original zone, resulting in 35 sub-zones compared to the five primary zones defined by the KGC framework (Tables 2, 3 and Appendix C). This refined classification was extended to other countries as follows: Egypt, from a single BWh climate zone to 7 sub-zones; Libya, from 3 zones (BSh, BWh, Csb) to 21 sub-zones; Tunisia, from 4 zones (Csa, BSh, BSk, BWh) to 28 sub-zones; Morocco, from 3 zones (Csa, BWh, BSh) to 21 sub-zones; and West Sahara, from a single BWh climate zone to 7 sub-zones.

It should be noted that the new climate sub-classifications are directly derived from the quantitative analysis of HDDs and CDDs for each studied region. These new ranges provide a more nuanced representation of local climatic zoning than the Köppen-Geiger classification alone.

Among the studied regions, Bordj Bou Arreridj in Algeria was identified as the coldest city, with annual HDD values reaching 2932 at a base temperature of 18 °C. Conversely, Adrar, also in Algeria, was found to be the hottest city, with annual CDD values amounting to 3169 at the same base temperature. These findings underscore the significant thermal energy demands of different regions, highlighting the need for tailored energy planning and building design strategies across North Africa.

5.2. Recommendations

The proposed tool delivers more precise results by utilizing ambient temperature data derived from the hourly NASA/POWER database, incorporating the altitude of the investigated cities. This approach significantly enhances the accuracy of climate zone delineations compared to the Köppen-Geiger classification (KGC), which primarily relies on ground cover as its primary metric. By addressing topographical influences, the tool overcomes the limitations of KGC in capturing localized climate variations.

In this regard, the current study covers a significantly larger geographic area compared to many previous studies conducted in Africa. For instance, researches by Idchabani et al, 2013 [58] and Conradie et al, 2015 [59] focused solely on the Moroccan, and South African territories, respectively, offering insights limited to a single country's climatic conditions. In contrast, this study extends its scope to a broader region, providing a more comprehensive analysis of heating and cooling degree-days across multiple territories specifically in North Africa. Furthermore, while the study conducted by Semahi et al, 2020 [60] identified nine new climate sub-zones in Algeria, the current study delineated 35 new sub-zones in Algeria, thereby offering a more detailed understanding of climate zones. Additionally, the study conducted by Abebe and Assefa, 2022 [85] mapped heating and cooling degree-days in Ethiopia, in Africa, using only two base temperatures: 21.8 °C for HDD and 23.8 °C for CDD. In comparison, the current study employs 12 base temperatures, enhancing its analytical depth and adaptability to various climatic and building conditions.

As an additional contribution, this study represents the first comprehensive analysis that simultaneously examines and maps building energy demands across the North African region. Within this area, HDDs range from 3 to 2932, while CDDs range from 1 to 3169, calculated using various base temperatures, resulting in a total of 119 new climate sub-classifications throughout the investigated area.

The findings of this study provide valuable insights for energy planning and building design. They enable the selection of optimal building elements, such as insulation thickness, window glazing types, and heating system capacities. These tailored recommendations enhance energy efficiency and thermal comfort across varying climate zones, ensuring that buildings are equipped to meet the specific energy demands of their respective regions.

Otherwise, future projections based on current trends can help to reveal climate change impacts on Heating Degree Day (HDD) and Cooling Degree Day (CDD) across North Africa. Drawing from global studies like Miranda et al. 2023 [57], which demonstrated substantial cooling demand increases, particularly within continental topographies, these regions will experience progressively higher cooling requirements. Thus, climate change scenarios predict a potential expansion of hot and arid zones in North Africa, potentially increasing cooling degree days by up to 20–30 %. These insights underscore the need for adaptive building thermal codes and regulations to mitigate increasing thermal stress and energy consumption.

It is recommended that architects, engineers, and building managers adopt this tool to improve indoor comfort and accurately estimate the building energy requirements. Furthermore, all building thermal requirements should be updated to align with the newly established climate classifications, ensuring compliance with local thermal regulations. These include the DTR C3-3 regulations in Algeria, the Housing and Building National Research Centre (HBRC) standards in Egypt, the Regulatory Thermal Code in Morocco (RTCM), and other relevant regulatory frameworks across the region. In this regard, implementing climate zoning refinement requires a multi-faceted steps. Key implementation strategies include mandatory energy efficiency assessments for new buildings, supporting retrofitting regional-specific thermal performance standards that account for diverse geographical contexts. A phased implementation approach, starting with pilot regions with more developed urban infrastructure, could provide scalable models for broader region adoption. Furthermore, it is necessary to create regular reporting mechanisms for thermal monitoring and evaluation, by implementing periodic review and update of climate zoning strategies. On the other hand, challenges include limited financial resources, variability in building stock age and quality, and the need for strong technical training among architects, engineers, and urban planners.

5.3. Strengths and limitations of this research

The research is underpinned by a vast dataset spanning 30 years (1989–2019), encompassing meteorological data from 108 weather stations across six North African geographic territories: Egypt, Libya, Tunisia, Algeria, Morocco, and Western Sahara. This extensive temporal and spatial coverage ensure a robust analysis of North Africa's diverse climatic conditions, accounting for variations in altitude, proximity to

Table 2
New KGC sub-classifications based on HDDs base temperatures in Algeri[a]a.

Cities	new KGC at 12 °C	new KGC at 14 °C	new KGC at 16 °C	new KGC at 18 °C	new KGC at 20 °C	new KGC at 22 °C
Ain Defla	Csa.1	Csa.2	Csa.2	Csa.4	Csa.5	Csa.7
Algiers	Csa.1	Csa.1	Csa.1	Csa.2	Csa.4	Csa.5
Annaba	Csa.1	Csa.1	Csa.2	Csa.3	Csa.4	Csa.5
Adrar	BWh.1	BWh.1	BWh.1	BWh.2	BWh.2	BWh.3
Ain Temouchent	Csa.2	Csa.3	Csa.5	Csa.6	Csa.7	Csa.7
Bordj Bou Arreridj	BSk.3	BSk.4	BSk.6	BSk.7	BSk.7	BSk.7
Bechar	BWk.1	BWk.2	BWk.2	BWk.3	BWk.4	BWk.5
Bejaia	Csa.2	Csa.3	Csa.4	Csa.6	Csa.7	Csa.7
Biskra	BWh.1	BWh.2	BWh.3	BWh.4	BWh.5	BWh.6
Batna	Cfa.2	Cfa.3	Cfa.5	Cfa.6	Cfa.7	Cfa.7
Chlef	Csa.1	Csa.2	Csa.3	Csa.4	Csa.5	Csa.7
Constantine	Csa.2	Csa.3	Csa.4	Csa.5	Csa.6	Csa.7
Djelfa	BSk.3	BSk.4	BSk.5	BSk.6	BSk.7	BSk.7
El Bayadh	BSk.3	BSk.3	BSk.5	BSk.6	BSk.7	BSk.7
El Oued	BWh.1	BWh.1	BWh.2	BWh.3	BWh.4	BWh.5
El Tarf	Csa.1	Csa.1	Csa.2	Csa.3	Csa.5	Csa.6
Guelma	Csa.2	Csa.2	Csa.3	Csa.5	Csa.6	Csa.7
Ghardaia	BWh.1	BWh.2	BWh.3	BWh.4	BWh.5	BWh.6
Illizi	BWh.1	BWh.1	BWh.1	BWh.2	BWh.3	BWh.4
Jijel	Csa.1	Csa.1	Csa.1	Csa.2	Csa.4	Csa.5
Laghouat	BWk.2	BWk.3	BWk.4	BWk.5	BWk.6	BWk.7
Mascara	Csa.2	Csa.3	Csa.4	Csa.5	Csa.6	Csa.7
Medea	Csa.1	Csa.2	Csa.3	Csa.4	Csa.5	Csa.7
Mostaganem	Csa.1	Csa.1	Csa.1	Csa.2	Csa.4	Csa.5
Msila	BWk.2	BWk.2	BWk.3	BWk.5	BWk.6	BWk.7
Naama	BWk.3	BWk.4	BWk.5	BWk.6	BWk.7	BWk.7
Oum El Bouaghi	Csa.2	Csa.3	Csa.5	Csa.6	Csa.7	Csa.7
Ouargla	BWk.1	BWk.1	BWk.2	BWk.3	BWk.4	BWk.5
Oran	Csa.1	Csa.1	Csa.2	Csa.3	Csa.4	Csa.6
Relizane	Csa.1	Csa.1	Csa.2	Csa.3	Csa.4	Csa.6
Souk Ahras	Csa.2	Csa.3	Csa.4	Csa.5	Csa.6	Csa.7
Sidi Bel Abbes	Csa.2	Csa.2	Csa.3	Csa.5	Csa.6	Csa.7
Saida	BSk.2	BSk.3	BSk.4	BSk.5	BSk.6	BSk.7
Setif	Csa.3	Csa.4	Csa.5	Csa.7	Csa.7	Csa.7
Skikda	Csa.1	Csa.1	Csa.2	Csa.3	Csa.4	Csa.6
Tebessa	BSk.3	BSk.4	BSk.5	BSk.6	BSk.7	BSk.7
Tlemcen	Csa.1	Csa.2	Csa.3	Csa.4	Csa.5	Csa.7
Tamanrasset	BWk.1	BWk.1	BWk.2	BWk.3	BWk.4	BWk.5
Tindouf	BWh.1	BWh.1	BWh.1	BWh.2	BWh.3	BWh.4
Tizi Ouzou	Csa.2	Csa.3	Csa.4	Csa.6	Csa.7	Csa.7
Tiaret	Csa.2	Csa.3	Csa.4	Csa.5	Csa.6	Csa.7
Climate scale	1	2	3	4	5	6	7
HDD quantities	< 300	300–600	600–900	900–1200	1200–1500	1500–1800	> 1800

[a] The given colors inside Tables 2, 3 and Appendix C are mandatory for data readability. Please, keep the colors as they are.

coastal areas, and desert regions. The inclusion of multiple climatic parameters, such as maximum and minimum temperatures, relative humidity, and wind speed, enhances the reliability of the findings and strengthens the conclusions drawn from the study.

By leveraging GIS-based spatial interpolation techniques, the study achieves a significant improvement in climate zoning resolution. It refines traditional classifications, increasing spatial detail from 12 321 km2 to 3025 km2 grids, enabling the identification of up to seven subzones per country. For example, Algeria's climate zones expanded from five general classifications to 35 detailed sub-classifications, capturing microclimatic variations that were previously overlooked. This high-resolution zoning bridges the gap between broad climate classifications and localized energy planning needs, making the findings particularly relevant for policymakers and urban planners.

The integration of Geographic Information Systems (GIS) with degree-day analysis provides a powerful framework for assessing and visualizing spatial variations in thermal energy demands. GIS tools enable the creation of precise and continuous climate maps, while degree-day calculations quantify heating degree days (HDD) and cooling degree days (CDD) across varying base temperatures. This combined approach ensures an accurate representation of regional energy needs, offering a robust analytical framework for identifying hotspots of heating or cooling demand and informing climate adaptation strategies.

The findings of this research translate into practical, actionable recommendations for the construction and energy sectors. By identifying regional heating and cooling demands with unprecedented accuracy, the study supports the development of tailored building codes, HVAC system designs, and energy efficiency policies. For instance, the data-driven insights enable recommendations for optimal insulation levels, glazing types, and HVAC set points based on specific sub-zone climatic conditions. These insights directly contribute to improving energy efficiency and thermal comfort in North Africa, addressing the region's unique energy and climatic challenges.The methodology developed in this research is highly adaptable, making it applicable to regions beyond North Africa with similar climatic diversity. The reliance on globally accessible datasets, such as NASA/POWER, and standardized GIS and degree-day analysis tools ensures that this approach can be replicated in other regions facing comparable energy planning challenges. By providing a framework for refining climate zoning and optimizing energy strategies, the study contributes to global sustainable development efforts, particularly in regions seeking to address climate change impacts and enhance energy resilience.

This study relied primarily on meteorological data from airport weather stations, as local urban weather files were not available. While the dataset provides robust regional coverage, incorporating urban weather files would have enhanced the analysis by accounting for urban heat island effects and the influence of urban morphology on microclimatic conditions. Despite this limitation, the research remains novel and

Table 3
New KGC sub-classifications based on CDDs base temperatures in Algeria.[a]

Cities	new KGC at 18 °C	new KGC at 20 °C	new KGC at 22 °C	new KGC at 24 °C	new KGC at 26 °C	new KGC at 28 °C
Ain Defla	Csa.4	Csa.3	Csa.2	Csa.1	Csa.1	Csa.1
Algiers	Csa.4	Csa.3	Csa.2	Csa.1	Csa.1	Csa.1
Annaba	Csa.4	Csa.3	Csa.2	Csa.1	Csa.1	Csa.1
Adrar	BWh.7	BWh.7	BWh.7	BWh.6	BWh.5	BWh.4
Ain Temouchent	Csa.4	Csa.4	Csa.2	Csa.1	Csa.1	Csa.1
Bordj Bou Arreridj	BSk.4	BSk.4	BSk.2	BSk.1	BSk.1	BSk.1
Bechar	BWk.7	BWk.6	BWk.5	BWk.4	BWk.3	BWk.2
Bejaia	Csa.3	Csa.2	Csa.2	Csa.1	Csa.1	Csa.1
Biskra	BWh.6	BWh.5	BWh.4	BWh.3	BWh.2	BWh.2
Batna	Cfa.3	Cfa.3	Cfa.2	Cfa.1	Cfa.1	Cfa.1
Chlef	Csa.5	Csa.4	Csa.3	Csa.2	Csa.1	Csa.1
Constantine	Csa.4	Csa.3	Csa.2	Csa.2	Csa.1	Csa.1
Djelfa	BSk.4	BSk.3	BSk.2	BSk.2	BSk.1	BSk.1
El Bayadh	BSk.4	BSk.3	BSk.2	BSk.2	BSk.1	BSk.1
El Oued	BWh.7	BWh.6	BWh.5	BWh.4	BWh.3	BWh.2
El Tarf	Csa.4	Csa.3	Csa.2	Csa.1	Csa.1	Csa.1
Guelma	Csa.4	Csa.3	Csa.2	Csa.2	Csa.1	Csa.1
Ghardaia	BWh.7	BWh.6	BWh.5	BWh.3	BWh.3	BWh.2
Illizi	BWh.7	BWh.7	BWh.6	BWh.5	BWh.4	BWh.3
Jijel	Csa.4	Csa.3	Csa.2	Csa.1	Csa.1	Csa.1
Laghouat	BWk.5	BWk.4	BWk.3	BWk.2	BWk.2	BWk.1
Mascara	Csa.4	Csa.3	Csa.2	Csa.2	Csa.1	Csa.1
Medea	Csa.4	Csa.3	Csa.2	Csa.1	Csa.1	Csa.1
Mostaganem	Csa.4	Csa.3	Csa.2	Csa.1	Csa.1	Csa.1
Msila	BWk.5	BWk.4	BWk.3	BWk.2	BWk.2	BWk.1
Naama	BWk.4	BWk.3	BWk.2	BWk.2	BWk.1	BWk.1
Oum El Bouaghi	Csa.3	Csa.3	Csa.2	Csa.1	Csa.1	Csa.1
Ouargla	BWk.7	BWk.7	BWk.6	BWk.4	BWk.3	BWk.3
Oran	Csa.4	Csa.3	Csa.2	Csa.1	Csa.1	Csa.1
Relizane	Csa.5	Csa.4	Csa.3	Csa.2	Csa.1	Csa.1
Souk Ahras	Csa.4	Csa.3	Csa.2	Csa.1	Csa.1	Csa.1
Sidi Bel Abbes	Csa.4	Csa.3	Csa.2	Csa.2	Csa.1	Csa.1
Saida	BSk.4	BSk.3	BSk.2	BSk.2	BSk.1	BSk.1
Setif	Csa.3	Csa.2	Csa.1	Csa.1	Csa.1	Csa.1
Skikda	Csa.4	Csa.3	Csa.2	Csa.1	Csa.1	Csa.1
Tebessa	BSk.3	BSk.2	BSk.2	BSk.1	BSk.1	BSk.1
Tlemcen	Csa.4	Csa.3	Csa.2	Csa.1	Csa.1	Csa.1
Tamanrasset	BWk.5	BWk.4	BWk.3	BWk.2	BWk.1	BWk.1
Tindouf	BWh.7	BWh.7	BWh.5	BWh.4	BWh.3	BWh.2
Tizi Ouzou	Csa.4	Csa.3	Csa.2	Csa.1	Csa.1	Csa.1
Tiaret	Csa.4	Csa.3	Csa.2	Csa.2	Csa.1	Csa.1
Climate scale	1	2	3	4	5	6	7
CDD quantities	< 300	300–600	600–900	900–1200	1200–1500	1500–1800	> 1800

[a] The given colors inside Tables 2, 3 and Appendix C are mandatory for data readability. Please, keep the colors as they are.

highly relevant, as it provides an empirical and realistic estimation of cooling and heating needs in North Africa.

The findings are particularly valuable for architects and policy-makers as they highlight the importance of designing climate-resilient buildings equipped with adequate cooling and heating systems, essential for mitigating the impacts of extreme weather conditions. This is especially critical for Northern Africa, a region plagued by fuel poverty, where energy-efficient retrofitting and climate-appropriate building design can significantly improve thermal comfort and reduce energy burdens for vulnerable populations.

5.4. Implications on practice and future work

This article introduces a novel approach that significantly enhances the realism and precision of energy use intensity (EUI) requirements for buildings in North Africa, paving the way for more effective strategies to achieve thermal comfort. By leveraging Heating Degree Days (HDD) and Cooling Degree Days (CDD) metrics at a high spatial resolution and incorporating altitude, this methodology provides a detailed understanding of regional thermal demands. These insights are critical for tailoring building energy requirements to specific climatic sub-zones, ensuring that energy consumption is aligned with actual environmental conditions.

The North African region faces unique challenges, including widespread fuel poverty and exposure to extreme climatic conditions such as heat waves and cold spells. Many buildings operate in "free-running mode," relying solely on passive measures for thermal comfort due to the high cost of heating and cooling systems. Additionally, a significant portion of occupants cannot afford to install two separate systems for cooling and heating, leaving them vulnerable during extreme weather events. This reality underscores the critical need for energy-efficient and climate-resilient building designs that minimize reliance on active systems while maximizing comfort and energy savings.

One of the key implications of this study is the necessity for building designers to develop a deeper understanding of local climate conditions. Rather than relying on generalized HVAC design practices based on the climatic conditions of a nation's capital, designers should account for the specific heating and cooling demands of the climatic zones identified

in this study. This localized approach enables the selection and sizing of HVAC systems that accurately reflect regional thermal demands, avoiding inefficiencies associated with a "one-size-fits-all" design philosophy.

The findings also emphasize the urgent need to update and enforce existing building standards across North Africa, such as the DTR C3-3 regulations in Algeria, the Housing and Building National Research Centre (HBRC) standards in Egypt, and the Regulatory Thermal Code in Morocco (RTCM). Current standards often fail to account for the significant microclimatic variations within these countries, resulting in over- or under-designed systems. By integrating the refined climate classifications presented in this study into building codes and enforcing them during building permit stages, stakeholders can ensure the construction of climate-proof buildings equipped with appropriate heating and cooling systems. These measures can alleviate energy burdens for vulnerable populations while enhancing resilience to extreme climatic events.

While this study provides a robust framework for climate classification and energy planning, future research should address certain limitations to further refine the methodology. Incorporating future climate change scenarios is imperative to account for the long-term impacts of global warming on thermal energy demands. Using future climate files, derived from global climate models, would enable the development of dynamic energy requirements that adapt to evolving climatic conditions, ensuring buildings remain resilient in the face of climate change.

Additionally, the inclusion of local urban weather files would provide a more nuanced understanding of microclimatic influences, such as urban heat islands and urban morphology. Urban weather files, which capture localized phenomena often overlooked by airport weather stations, are critical for accurately modeling energy demands in densely populated areas. Future studies should also explore the integration of real-time climate monitoring with adaptive building technologies to optimize energy use dynamically.

By addressing these areas, future research can expand the applicability of this approach, ensuring that building energy standards in North Africa and other regions with similar climatic challenges remain robust, forward-looking, and effective in achieving both thermal comfort and energy efficiency.

6. Conclusion

This study presents a data-driven methodology refining climate zoning in North Africa using 30 years of meteorological data from 108 weather stations across six geographic territories. By leveraging Heating Degree Days (HDD) and Cooling Degree Days (CDD) at multiple base temperatures, the research improves zoning resolution from 12 321 km^2 to 3025 km^2. This detailed approach identified up to seven sub-classifications per territory, with Algeria alone expanding from five to 35 sub-zones.

The findings reveal thermal energy demand variations across the region. The coldest city, Bordj Bou Arreridj, recorded annual HDDs of 2932 at 18 °C, while the hottest city, Adrar, exhibited annual CDDs of 3169. Overall, HDDs range from 3 to 2932, while CDDs range from 1 to 3169, highlighting diverse building energy requirements. These extremes demonstrate the need for location-specific building codes in a region characterized by fuel poverty and reliance on free-running buildings.

This comprehensive study moves beyond traditional categorizations by integrating meteorological data with GIS modeling to create nuanced climate zones. This enables architects and engineers to develop location-specific energy solutions and optimized building design. The high-resolution spatial analysis establishes a precise framework for regional energy mapping, impacting thermal regulations and energy efficiency standards.

This research offers actionable data for climate-resilient building designs tailored to local demands. It also establishes a foundation for future research incorporating urban weather files and climate change scenarios.

On the other hand, the study needs dynamic climate change projections. Future work should integrate high-resolution urban weather data, develop machine learning algorithms for predictive energy modeling, and explore nuanced climate change scenarios to enhance adaptive building energy strategies in North Africa.

CRediT authorship contribution statement

Mohamed Elhadi Matallah: Writing – review & editing, Writing – original draft, Visualization, Validation, Software, Methodology, Investigation, Formal analysis, Data curation, Conceptualization. **Andreas Matzarakis:** Writing – review & editing, Validation, Supervision, Methodology. **Aissa Boulkaibet:** Writing – review & editing, Writing – original draft, Visualization, Validation, Software, Formal analysis, Data curation. **Atef Ahriz:** Writing – review & editing, Validation, Resources, Methodology, Formal analysis, Conceptualization. **Dyna Chourouk Zitouni:** Writing – review & editing, Software, Formal analysis. **Fatima Zahra Ben Ratmia:** Writing – review & editing, Visualization, Validation, Data curation. **Waqas Ahmed Mahar:** Writing – review & editing, Software, Resources, Methodology, Data curation. **Faten Ghanemi:** Writing – review & editing, Writing – original draft, Validation. **Shady Attia:** Writing – review & editing, Validation, Supervision, Resources, Methodology, Conceptualization.

Declaration of competing interest

The authors declare that they have no known competing financial interests or personal relationships that could have appeared to influence the work reported in this paper.

Acknowledgement

We would like to acknowledge the LARGHYDE Laboratory, University of Biskra, and the Sustainable Building Design (SBD) Laboratory, at the University of Liege, Belgium for their valuable support during the experiments and data analysis. The authors would also like to thank the University of Biskra, Algeria and the University of Liege, Belgium for their assistance in administrative procedures.

Appendix A

.

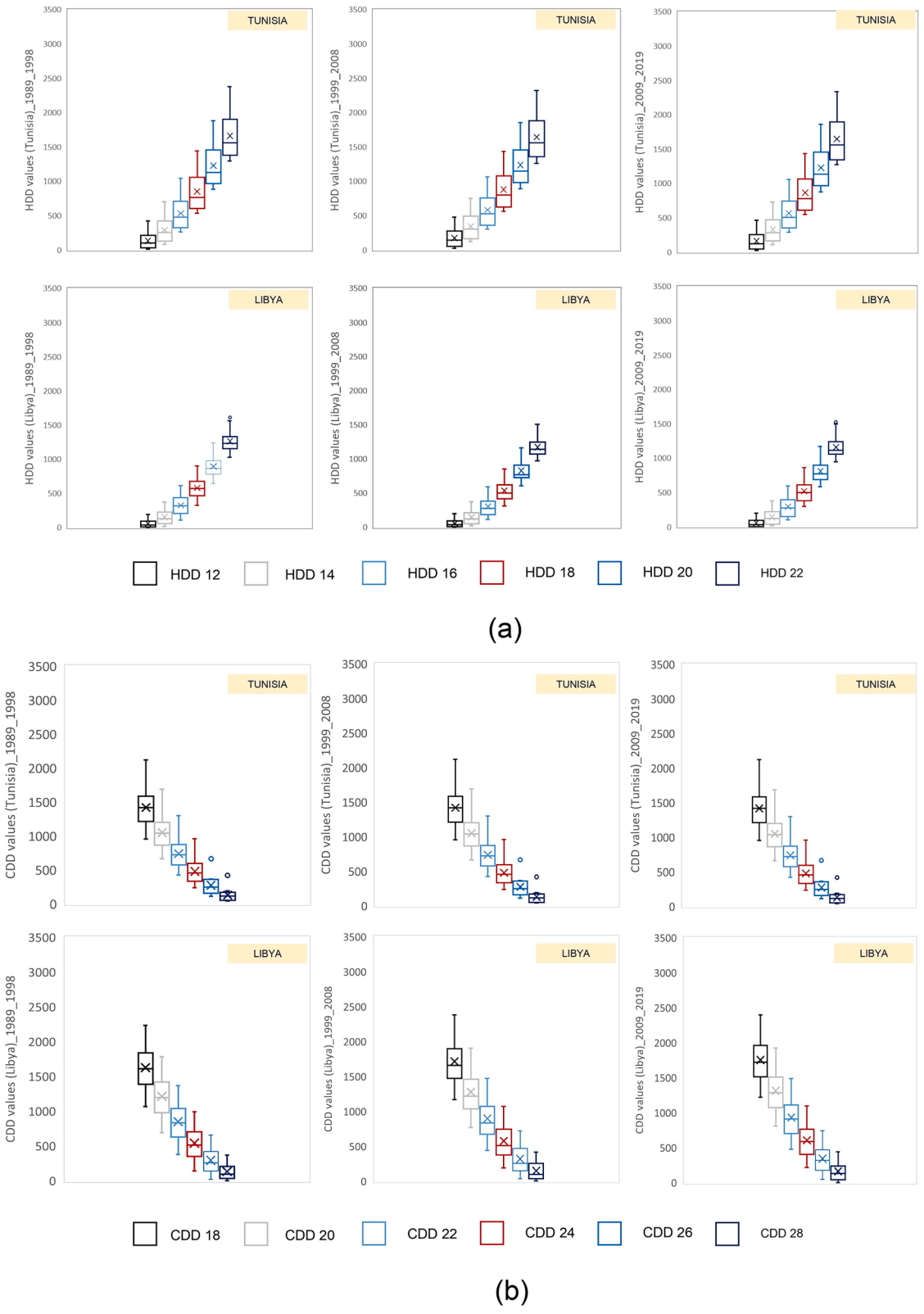

Fig. A1. Box plots of heating and cooling demands during three decades within the studied area: (a) comparative HDD quantities between Tunisia and Libya; (b) comparative CDD quantities between Tunisia and Libya.

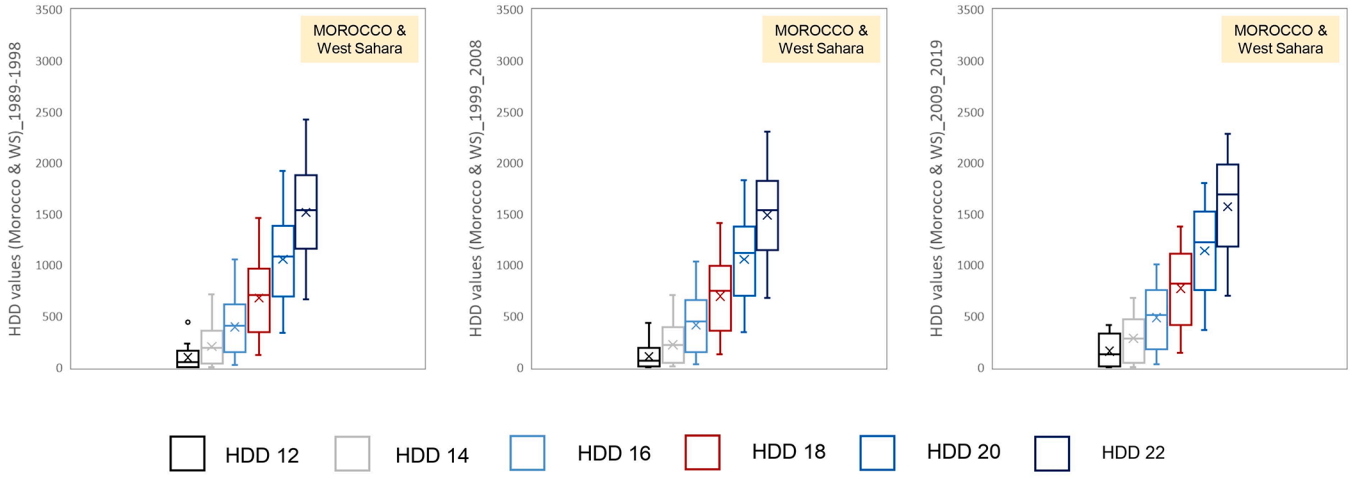

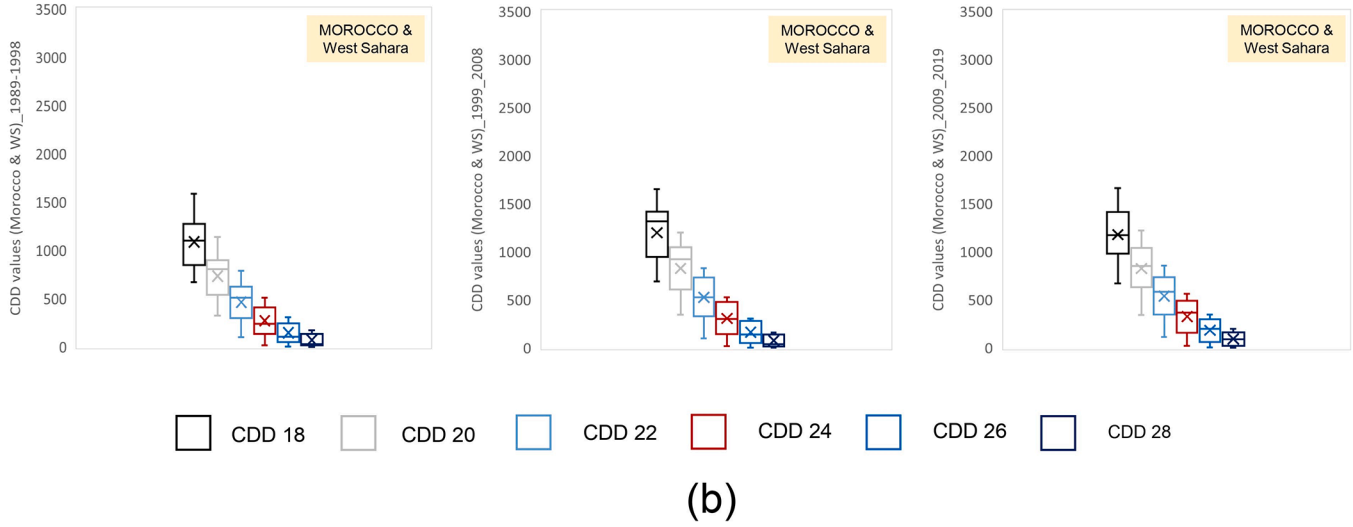

Fig. A2. Box plots of heating and cooling demands during three decades within the studied area: (a) comparative HDD quantities between Morocco and Western Sahara; (b) comparative CDD quantities between Morocco and Western Sahara.

Appendix B

.

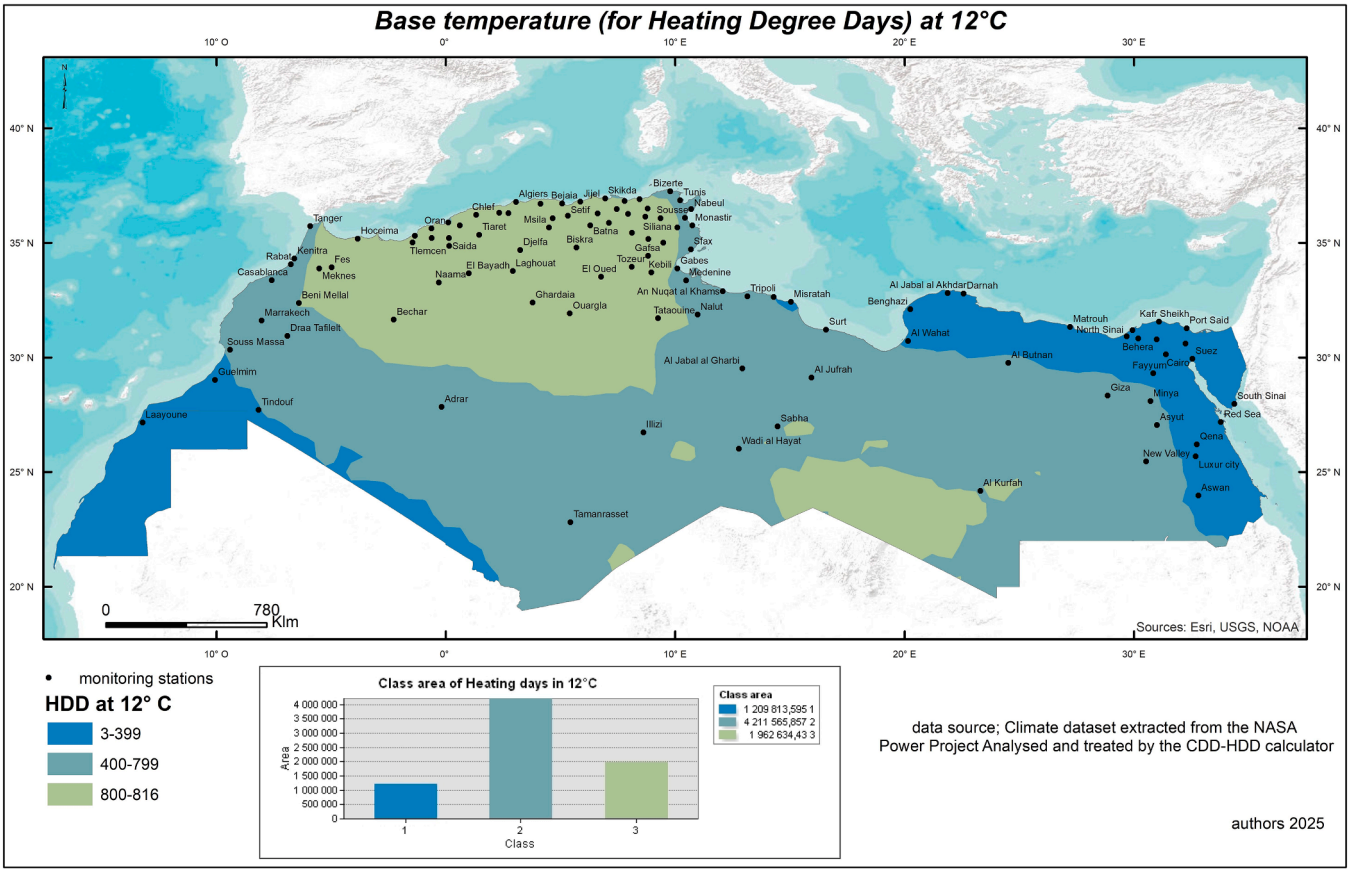

Fig. B1. HDDs map within the investigated countries in North Africa: at 12 °C base temperature.

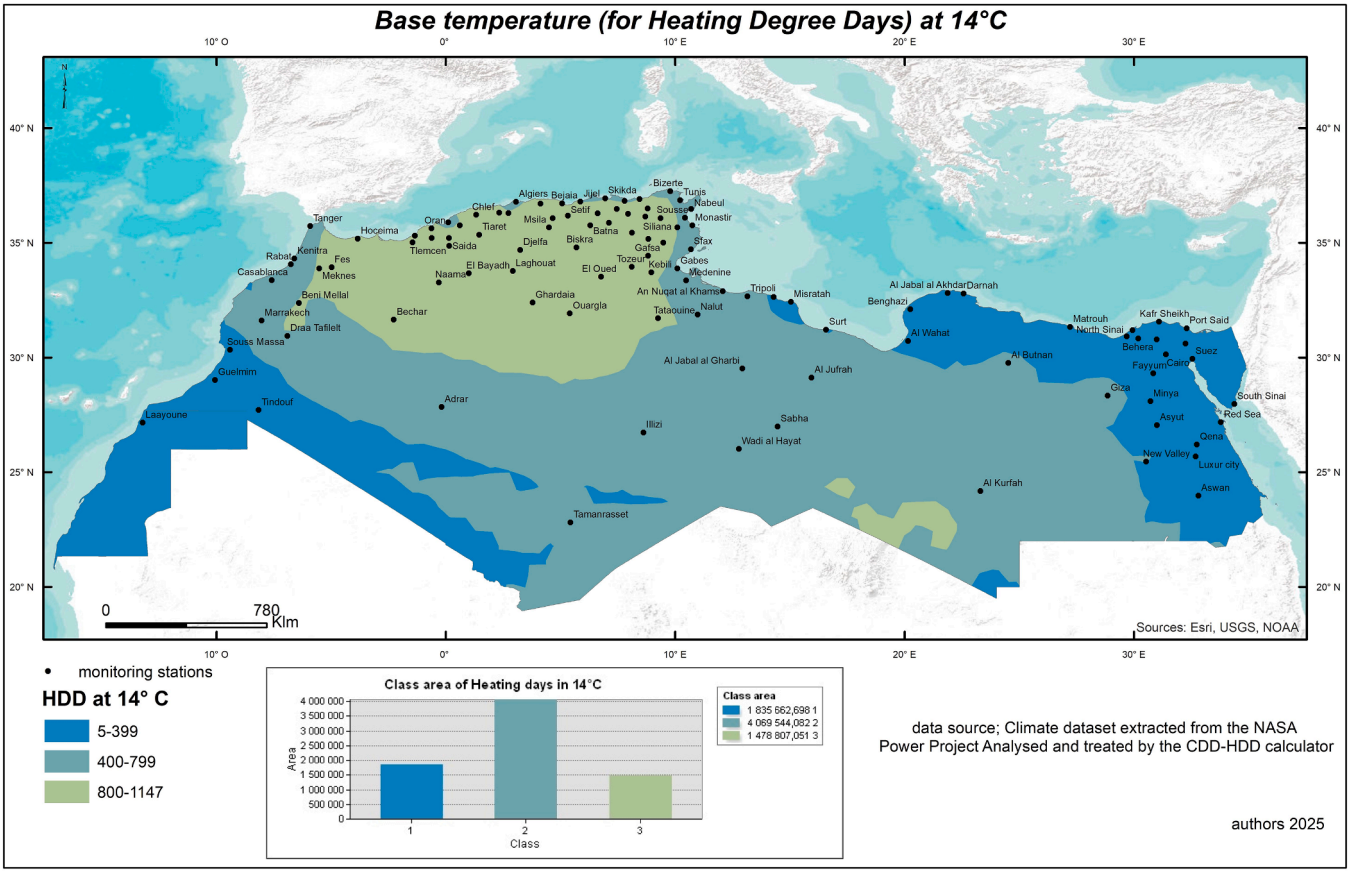

Fig. B2. HDDs map within the investigated countries in North Africa: at 14 °C base temperature.

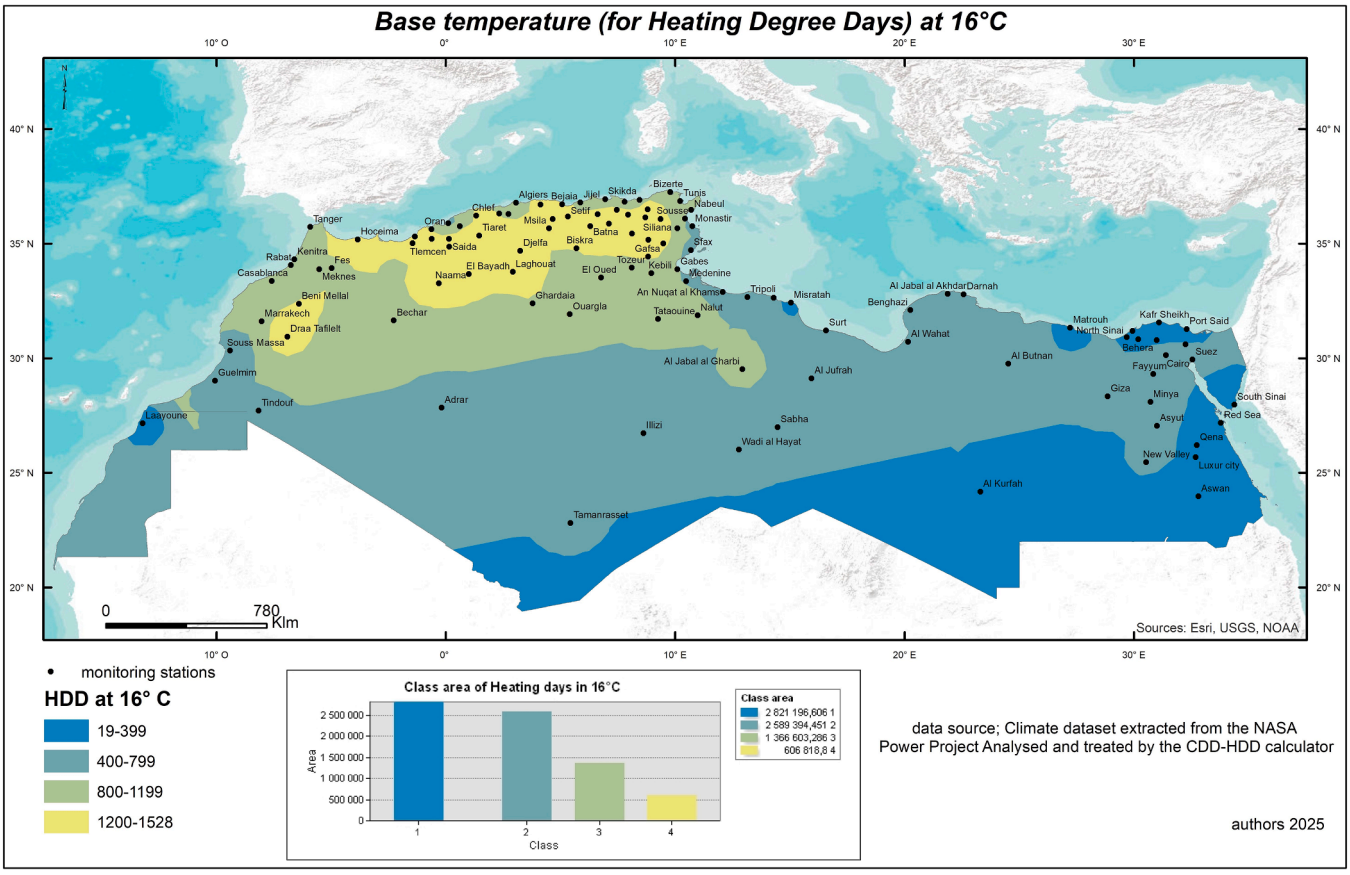

Fig. B3. HDDs map within the investigated countries in North Africa: at 16 °C base temperature.

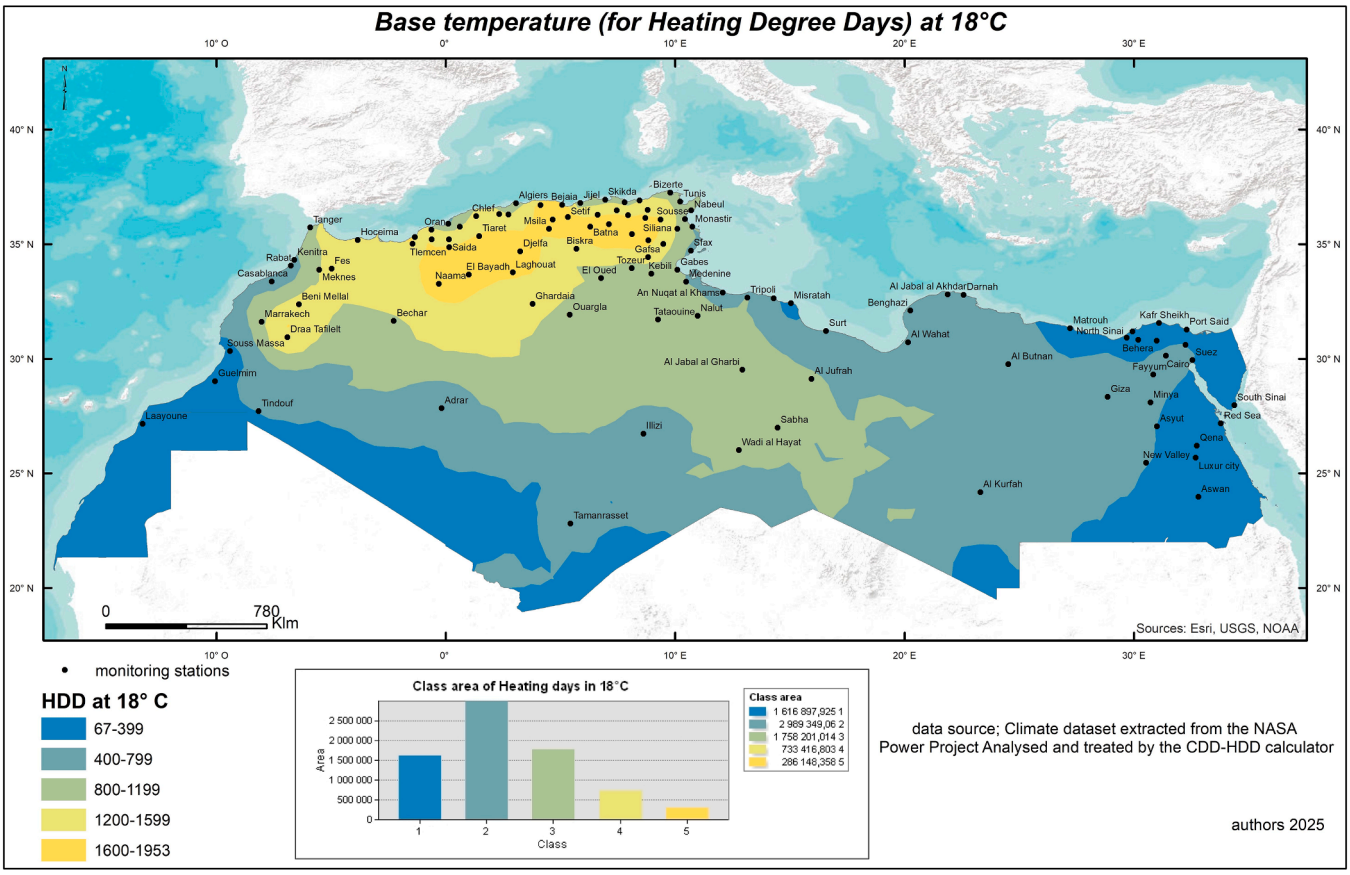

Fig. B4. HDDs map within the investigated countries in North Africa: at 18 °C base temperature.

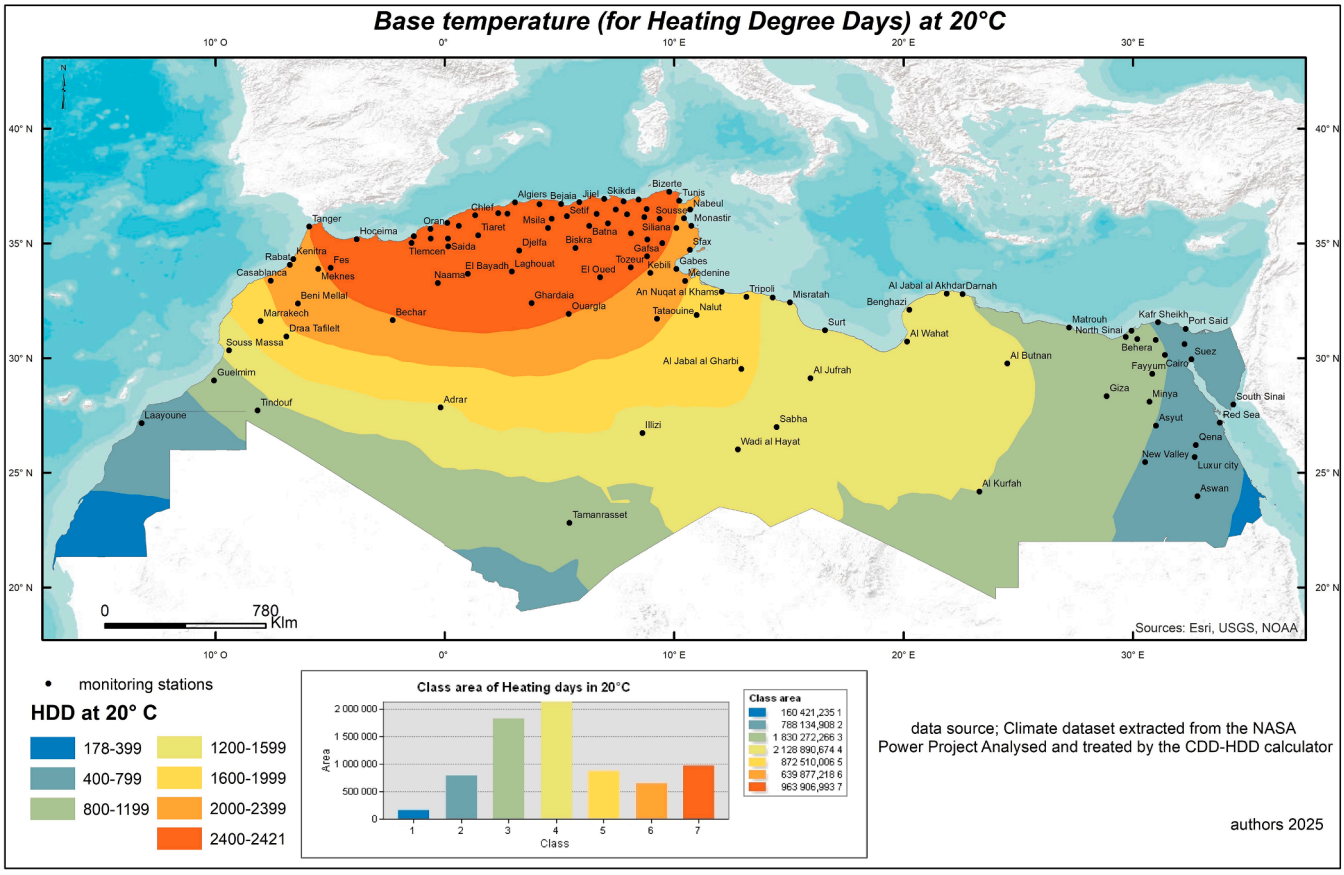

Fig. B5. HDDs map within the investigated countries in North Africa: at 20 °C base temperature.

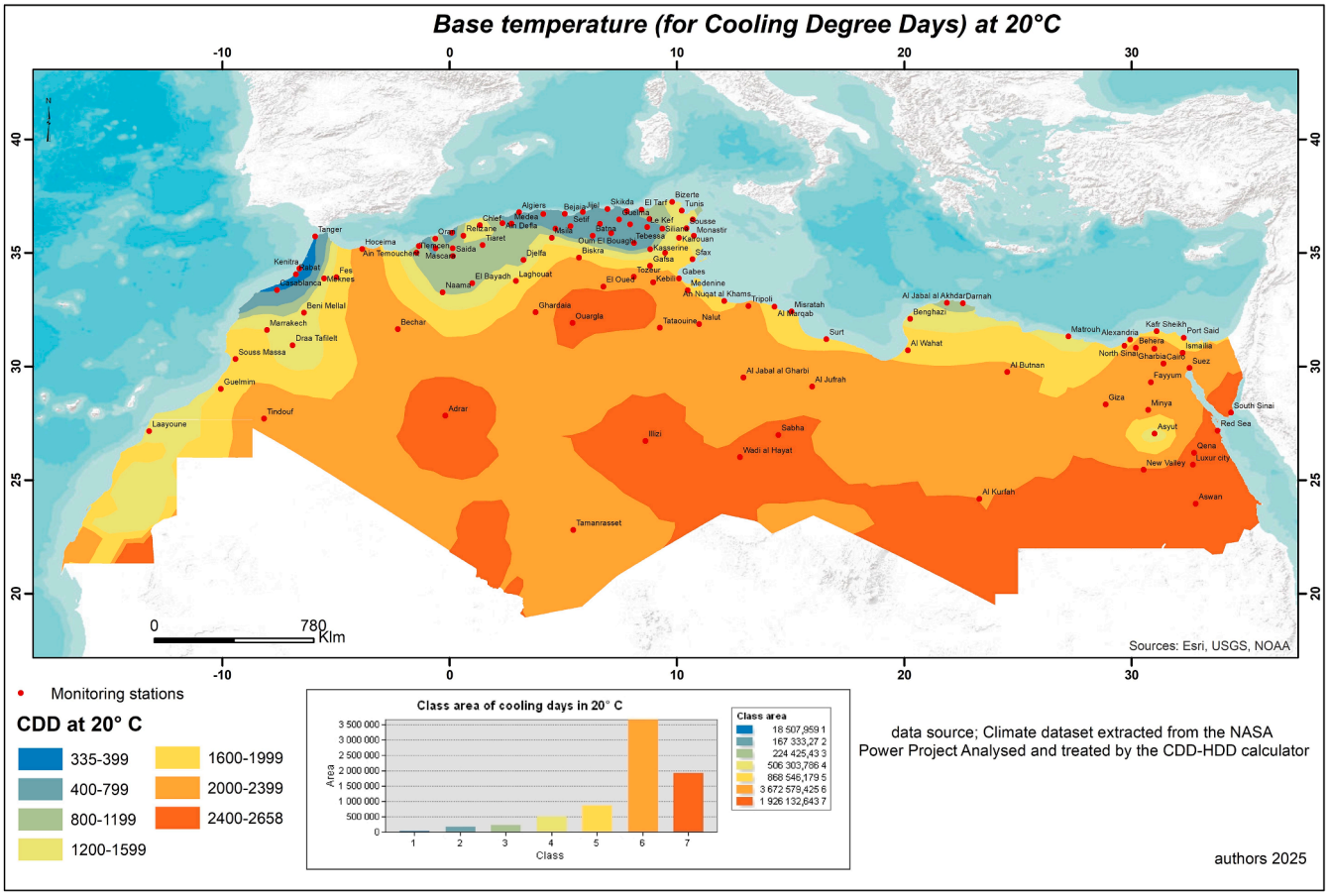

Fig. B6. CDDs map within the investigated countries in North Africa: at 20 °C base temperature.

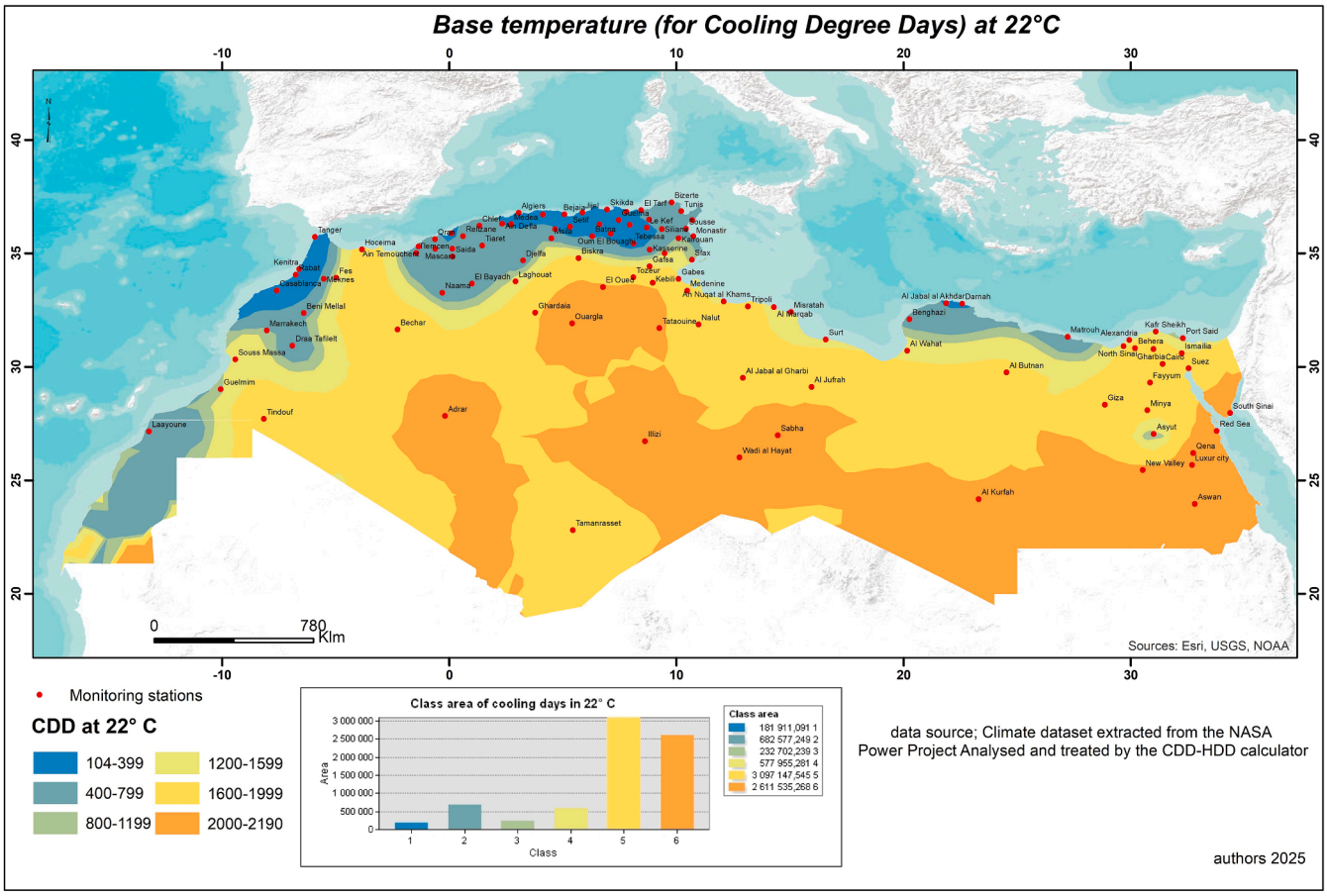

Fig. B7. CDDs map within the investigated countries in North Africa: at 22 °C base temperature.

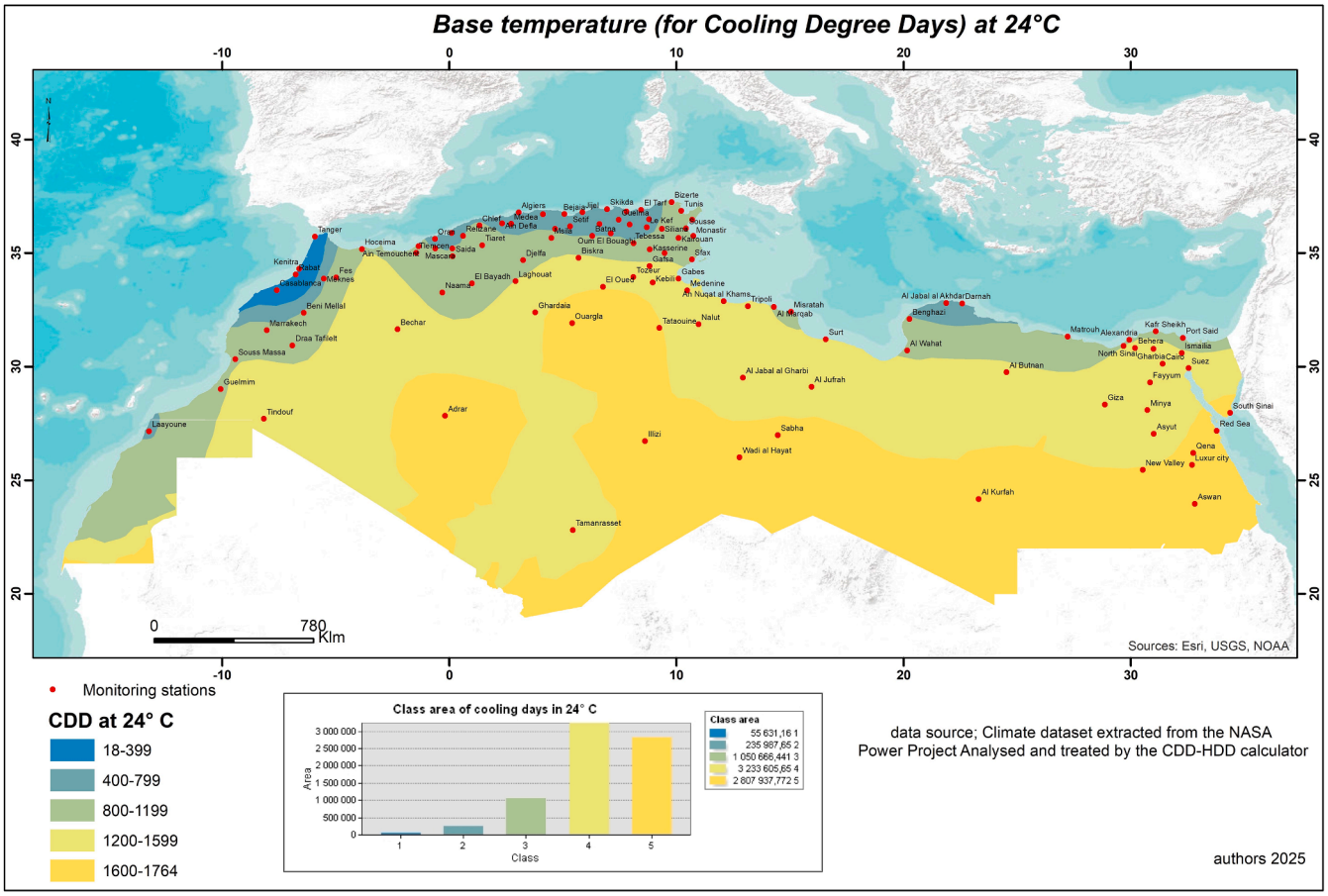

Fig. B8. CDDs map within the investigated countries in North Africa: at 24 °C base temperature.

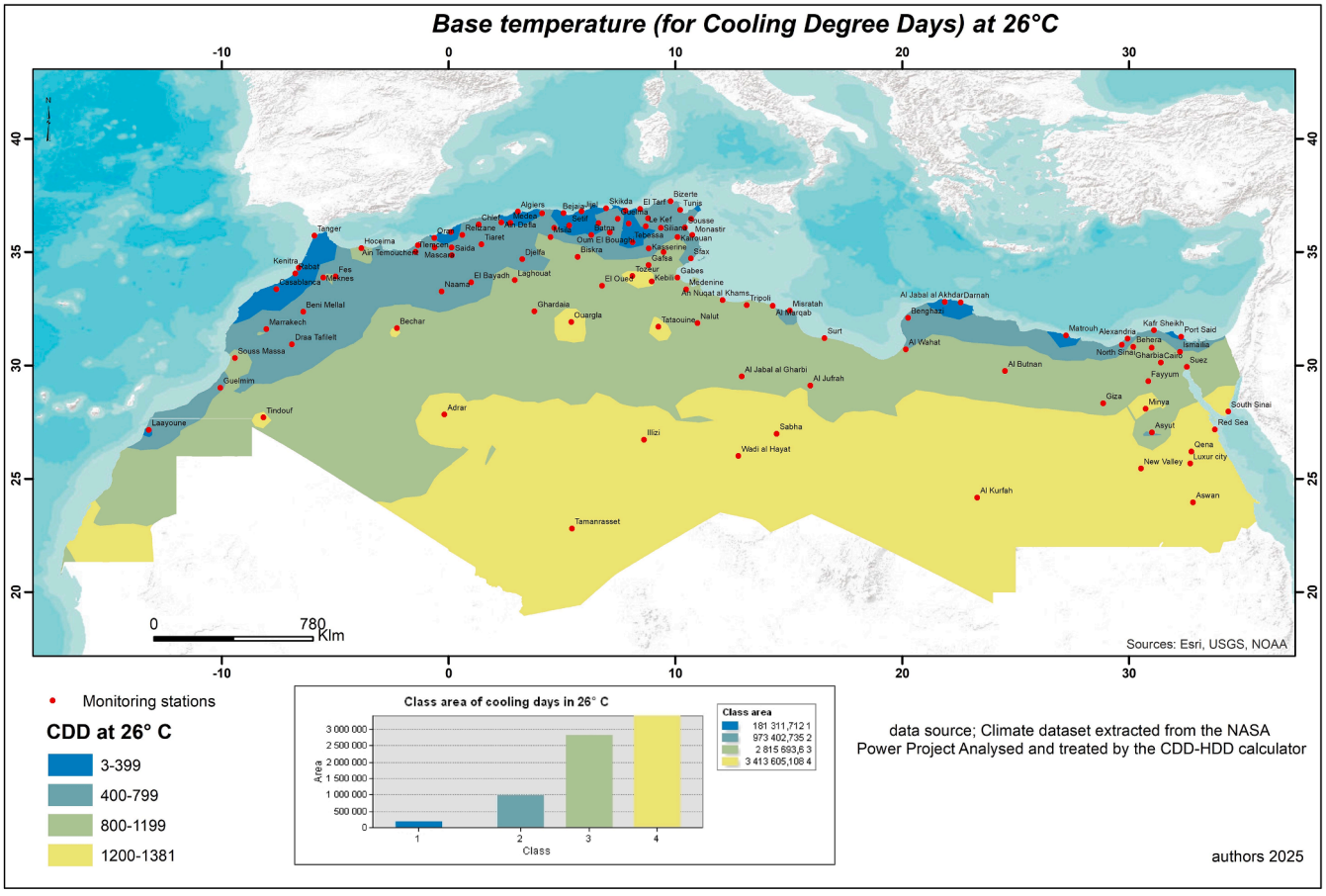

Fig. B9. CDDs map within the investigated countries in North Africa: at 26 °C base temperature.

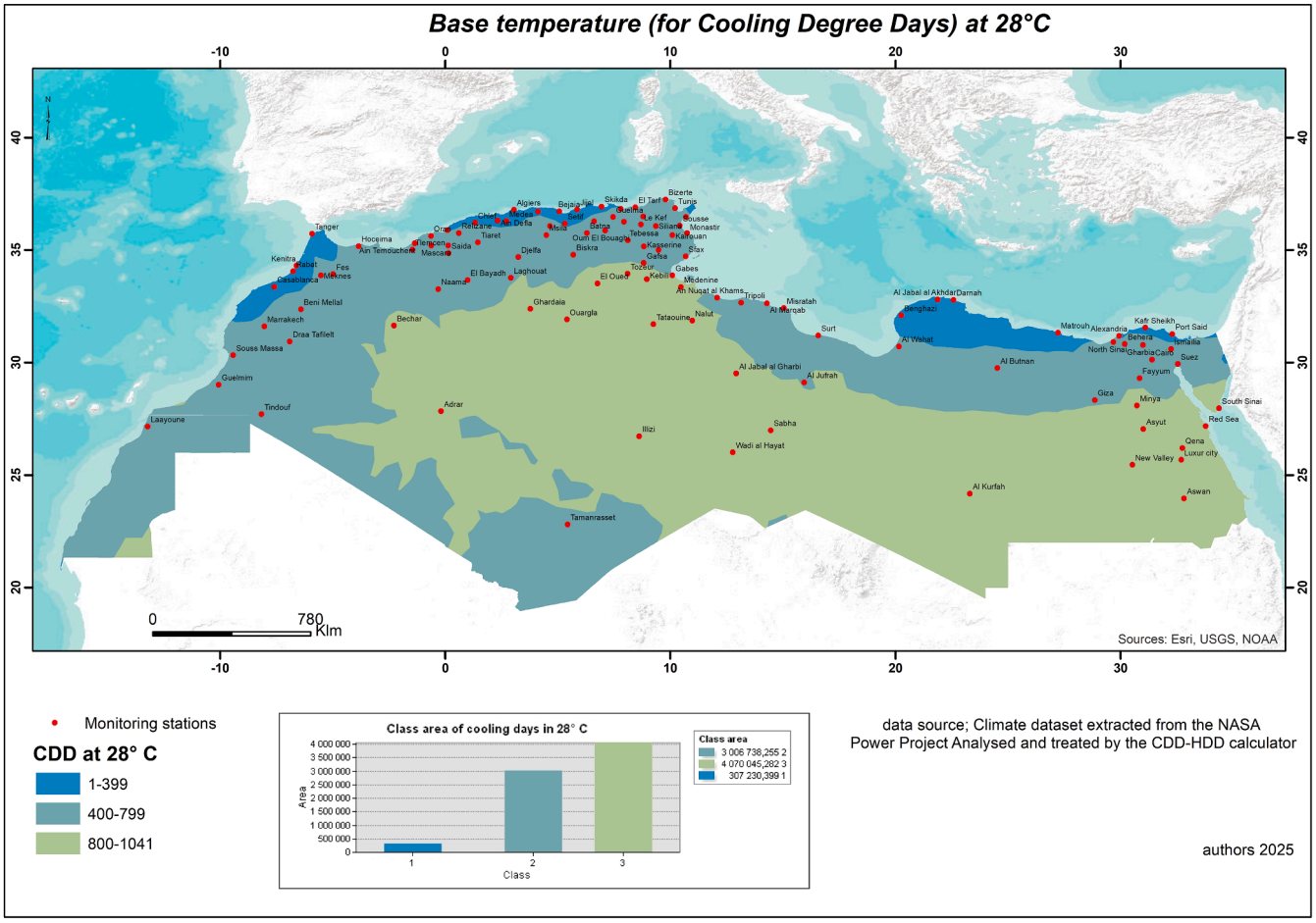

Fig. B10. CDDs map within the investigated countries in North Africa: at 28 °C base temperature.

Appendix C

.

Table C1
New KGC sub-classifications based on HDDs base temperatures in Morocco and Western Sahara.[a]

Cities	new KGC at 12 °C	new KGC at 14 °C	new KGC at 16 °C	new KGC at 18 °C	new KGC at 20 °C	new KGC at 22 °C
Beni Mellal	Csa.1	Csa.2	Csa.3	Csa.4	Csa.6	Csa.7
Casablanca	Csa.1	Csa.1	Csa.1	Csa.2	Csa.3	Csa.5
Draa Tafilelt	Csa.2	Csa.3	Csa.4	Csa.5	Csa.7	Csa.7
Fes	Csa.1	Csa.2	Csa.2	Csa.3	Csa.5	Csa.6
Guelmim	BWh.1	BWh.1	BWh.1	BWh.2	BWh.3	BWh.4
Marrakech	BSh.1	BSh.1	BSh.2	BSh.3	BSh.4	BSh.6
Rabat	Csa.1	Csa.1	Csa.1	Csa.2	Csa.3	Csa.5
Souss Massa	Csa.1	Csa.1	Csa.1	Csa.2	Csa.3	Csa.4
Tanger	Csa.1	Csa.1	Csa.2	Csa.3	Csa.5	Csa.6
Meknes	Csa.1	Csa.2	Csa.2	Csa.3	Csa.5	Csa.6
Kenitra	Csa.1	Csa.1	Csa.1	Csa.2	Csa.4	Csa.5
Hoceima	Csa.1	Csa.2	Csa.3	Csa.4	Csa.6	Csa.7
Laayoune (W. S)	BWh.1	BWh.1	BWh.1	BWh.1	BWh.2	BWh.3
Climate scale	1	2	3	4	5	6	7
HDD quantities	< 300	300–600	600–900	900–1200	1200–1500	1500–1800	> 1800

[a] The given colors inside Tables 2, 3 and Appendix C are mandatory for data readability. Please, keep the colors as they are.

Table C2
New KGC sub-classifications based on CDDs base temperatures in Morocco and Western Sahara.

Cities	new KGC at 18 °C	new KGC at 20 °C	new KGC at 22 °C	new KGC at 24 °C	new KGC at 26 °C	new KGC at 28 °C
Beni Mellal	Csa.5	Csa.4	Csa.3	Csa.2	Csa.1	Csa.1
Casablanca	Csa.4	Csa.2	Csa.2	Csa.1	Csa.1	Csa.1
Draa Tafilelt	Csa.4	Csa.3	Csa.2	Csa.1	Csa.1	Csa.1
Fes	Csa.5	Csa.4	Csa.3	Csa.2	Csa.1	Csa.1
Guelmim	BWh.5	BWh.4	BWh.3	BWh.2	BWh.1	BWh.1
Marrakech	BSh.5	BSh.4	BSh.3	BSh.2	BSh.1	BSh.1
Rabat	Csa.4	Csa.2	Csa.1	Csa.1	Csa.1	Csa.1
Souss Massa	Csa.6	Csa.4	Csa.3	Csa.2	Csa.2	Csa.1
Tanger	Csa.4	Csa.3	Csa.2	Csa.1	Csa.1	Csa.1
Meknes	Csa.5	Csa.4	Csa.3	Csa.2	Csa.1	Csa.1
Kenitra	Csa.3	Csa.2	Csa.1	Csa.1	Csa.1	Csa.1
Hoceima	Csa.7	Csa.6	Csa.4	Csa.3	Csa.2	Csa.1
Laayoune (W. S)	BWh.5	BWh.4	BWh.2	BWh.1	BWh.2	BWh.1
Climate scale	1	2	3	4	5	6	7
CDD quantities	< 300	300–600	600–900	900–1200	1200–1500	1500–1800	> 1800

Table C3
New KGC sub-classifications based on HDDs base temperatures in Egypt.

Cities	new KGC at 12 °C	new KGC at 14 °C	new KGC at 16 °C	new KGC at 18 °C	new KGC at 20 °C	new KGC at 22 °C
Aswan	BWh.1	BWh.1	BWh.1	BWh.1	BWh.2	BWh.2
Asyut	BWh.1	BWh.1	BWh.1	BWh.2	BWh.3	BWh.4
Red Sea	BWh.1	BWh.1	BWh.1	BWh.1	BWh.2	BWh.3
Behera	BWh.1	BWh.1	BWh.1	BWh.2	BWh.2	BWh.4
Port Said	BWh.1	BWh.1	BWh.1	BWh.1	BWh.2	BWh.3
Fayyum	BWh.1	BWh.1	BWh.1	BWh.2	BWh.3	BWh.4
Gharbia	BWh.1	BWh.1	BWh.1	BWh.2	BWh.2	BWh.3
Alexandria	BWh.1	BWh.1	BWh.1	BWh.2	BWh.2	BWh.4
Ismailia	BWh.1	BWh.1	BWh.1	BWh.2	BWh.3	BWh.4
South Sinai	BWh.1	BWh.1	BWh.1	BWh.1	BWh.1	BWh.2
Giza	BWh.1	BWh.1	BWh.2	BWh.2	BWh.3	BWh.5
Kafr Sheikh	BWh.1	BWh.1	BWh.1	BWh.1	BWh.2	BWh.3
Minya	BWh.1	BWh.1	BWh.1	BWh.2	BWh.3	BWh.4
Matrouh	BWh.1	BWh.1	BWh.1	BWh.1	BWh.2	BWh.4
Cairo	BWh.1	BWh.1	BWh.1	BWh.2	BWh.3	BWh.4
Qena	BWh.1	BWh.1	BWh.1	BWh.1	BWh.2	BWh.3
North Sinai	BWh.1	BWh.1	BWh.1	BWh.2	BWh.2	BWh.4
Suez	BWh.1	BWh.1	BWh.1	BWh.2	BWh.3	BWh.4
Luxur city	BWh.1	BWh.1	BWh.1	BWh.2	BWh.2	BWh.3
New Valley	BWh.1	BWh.1	BWh.1	BWh.2	BWh.3	BWh.4
Climate scale	1	2	3	4	5	6	7
HDD quantities	< 300	300–600	600–900	900–1200	1200–1500	1500–1800	> 1800

Table C4
New KGC sub-classifications based on CDDs base temperatures in Egypt.

Cities	new KGC at 18 °C	new KGC at 20 °C	new KGC at 22 °C	new KGC at 24 °C	new KGC at 26 °C	new KGC at 28 °C
Aswan	BWh.7	BWh.7	BWh.7	BWh.6	BWh.4	BWh.3
Asyut	BWh.4	BWh.3	BWh.2	BWh.1	BWh.1	BWh.1
Red Sea	BWh.7	BWh.7	BWh.5	BWh.4	BWh.3	BWh.2
Behera	BWh.6	BWh.5	BWh.3	BWh.2	BWh.1	BWh.1
Port Said	BWh.5	BWh.4	BWh.2	BWh.1	BWh.1	BWh.1
Fayyum	BWh.7	BWh.6	BWh.4	BWh.3	BWh.2	BWh.1
Gharbia	BWh.7	BWh.6	BWh.4	BWh.3	BWh.2	BWh.1

(*continued on next page*)

Table C4 (*continued*)

Cities	new KGC at 18 °C	new KGC at 20 °C	new KGC at 22 °C	new KGC at 24 °C	new KGC at 26 °C	new KGC at 28 °C
Alexandria	BWh.6	BWh.5	BWh.3	BWh.2	BWh.1	BWh.1
Ismailia	BWh.7	BWh.5	BWh.4	BWh.3	BWh.2	BWh.1
South Sinai	BWh.7	BWh.7	BWh.7	BWh.5	BWh.4	BWh.2
Giza	BWh.7	BWh.5	BWh.4	BWh.3	BWh.1	BWh.1
Kafr Sheikh	BWh.6	BWh.4	BWh.3	BWh.2	BWh.2	BWh.1
Minya	BWh.7	BWh.6	BWh.5	BWh.4	BWh.2	BWh.2
Matrouh	BWh.5	BWh.3	BWh.2	BWh.1	BWh.1	BWh.1
Cairo	BWh.7	BWh.6	BWh.4	BWh.3	BWh.2	BWh.1
Qena	BWh.7	BWh.7	BWh.6	BWh.5	BWh.4	BWh.2
North Sinai	BWh.6	BWh.5	BWh.3	BWh.2	BWh.1	BWh.1
Suez	BWh.7	BWh.5	BWh.4	BWh.3	BWh.2	BWh.1
Luxur city	BWh.7	BWh.7	BWh.6	BWh.5	BWh.3	BWh.2
New Valley	BWh.7	BWh.7	BWh.5	BWh.4	BWh.3	BWh.2
Climate scale	1	2	3	4	5	6	7
CDD quantities	< 300	300–600	600–900	900–1200	1200–1500	1500–1800	> 1800

Table C5
New KGC sub-classifications based on HDDs base temperatures in Libya.

Cities	new KGC at 12 °C	new KGC at 14 °C	new KGC at 16 °C	new KGC at 18 °C	new KGC at 20 °C	new KGC at 22 °C
Benghazi	BSh.1	BSh.1	BSh.1	BSh.2	BSh.3	BSh.4
Al Butnan	BWh.1	BWh.1	BWh.2	BWh.3	BWh.4	BWh.5
Darnah	BSh.1	BSh.1	BSh.1	BSh.2	BSh.3	BSh.4
Al Jabal al Akhdar	Csb.1	Csb.1	Csb.1	Csb.2	Csb.3	Csb.4
Al Jabal al Gharbi	BSh.1	BSh.2	BSh.3	BSh.3	BSh.4	BSh.6
Al Jufrah	BWh.1	BWh.1	BWh.2	BWh.3	BWh.4	BWh.5
Al Kurfah	BWh.1	BWh.1	BWh.2	BWh.2	BWh.2	BWh.4
Al Marqab	BSh.1	BSh.1	BSh.1	BSh.2	BSh.3	BSh.4
Misratah	BSh.1	BSh.1	BSh.1	BSh.2	BSh.3	BSh.4
Nalut	BWh.1	BWh.2	BWh.2	BWh.3	BWh.4	BWh.6
An Nuqat al Khams	BWh.1	BWh.1	BWh.1	BWh.2	BWh.3	BWh.4
Sabha	BWh.1	BWh.1	BWh.2	BWh.3	BWh.3	BWh.4
Surt	BWh.1	BWh.1	BWh.1	BWh.2	BWh.3	BWh.4
Tripoli	BSh.1	BSh.1	BSh.2	BSh.3	BSh.4	BSh.5
Al Wahat	BWh.1	BWh.1	BWh.1	BWh.2	BWh.3	BWh.4
Wadi al Hayat	BWh.1	BWh.1	BWh.2	BWh.3	BWh.3	BWh.4
Climate scale	1	2	3	4	5	6	7
HDD quantities	< 300	300–600	600–900	900–1200	1200–1500	1500–1800	> 1800

Table C6
New KGC sub-classifications based on CDDs base temperatures in Libya.

Cities	new KGC at 18°C	new KGC at 20°C	new KGC at 22°C	new KGC at 24 °C	new KGC at 26 °C	new KGC at 28 °C
Benghazi	BSh.5	BSh.4	BSh.2	BSh.1	BSh.1	BSh.1
Al Butnan	BWh.6	BWh.5	BWh.4	BWh.3	BWh.2	BWh.1
Darnah	BSh.4	BSh.3	BSh.2	BSh.1	BSh.1	BSh.1
Al Jabal al Akhdar	Csb.5	Csb.3	Csb.2	Csb.1	Csb.1	Csb.1
Al Jabal al Gharbi	BSh.6	BSh.5	BSh.4	BSh.3	BSh.2	BSh.1
Al Jufrah	BWh.7	BWh.6	BWh.4	BWh.3	BWh.2	BWh.1
Al Kurfah	BWh.7	BWh.6	BWh.5	BWh.4	BWh.2	BWh.1
Al Marqab	BSh.6	BSh.4	BSh.3	BSh.2	BSh.1	BSh.1

(*continued on next page*)

Table C6 (*continued*)

Cities	new KGC at 18°C	new KGC at 20°C	new KGC at 22°C	new KGC at 24 °C	new KGC at 26 °C	new KGC at 28 °C
Misratah	BSh.5	BSh.4	BSh.3	BSh.2	BSh.1	BSh.1
Nalut	BWh.6	BWh.5	BWh.4	BWh.3	BWh.2	BWh.1
An Nuqat al Khams	BWh.6	BWh.4	BWh.3	BWh.2	BWh.1	BWh.1
Sabha	BWh.7	BWh.7	BWh.5	BWh.4	BWh.3	BWh.2
Surt	BWh.6	BWh.4	BWh.3	BWh.2	BWh.1	BWh.1
Tripoli	BSh.7	BSh.5	BSh.4	BSh.3	BSh.2	BSh.1
Al Wahat	BWh.6	BWh.4	BWh.3	BWh.2	BWh.1	BWh.1
Wadi al Hayat	BWh.7	BWh.7	BWh.5	BWh.4	BWh.3	BWh.2
Climate scale	1	2	3	4	5	6	7
CDD quantities	< 300	300–600	600–900	900–1200	1200–1500	1500–1800	> 1800

Table C7
New KGC sub-classifications based on HDDs base temperatures in Tunisia.

Cities	new KGC at 12 °C	new KGC at 14 °C	new KGC at 16 °C	new KGC at 18 °C	new KGC at 20 °C	new KGC at 22 °C
Bizerte	Csa.1	Csa.1	Csa.2	Csa.3	Csa.4	Csa.6
Gabes	BWh.1	BWh.1	BWh.2	BWh.3	BWh.4	BWh.5
Gafsa	BWh.1	BWh.2	BWh.3	BWh.4	BWh.5	BWh.7
Jendouba	Csa.1	Csa.2	Csa.3	Csa.4	Csa.6	Csa.7
Kebili	BWh.1	BWh.1	BWh.2	BWh.3	BWh.4	BWh.5
Le Kef	BSk.2	BSk.3	BSk.4	BSk.5	BSk.7	BSk.7
Kairouan	BSh.1	BSh.2	BSh.2	BSh.3	BSh.4	BSh.6
Kasserine	BSk.2	BSk.3	BSk.4	BSk.5	BSk.7	BSk.7
Medenine	BSh.1	BSh.1	BSh.2	BSh.3	BSh.4	BSh.5
Monastir	Bsh.1	Bsh.1	Bsh.2	Bsh.3	Bsh.4	Bsh.5
Nabeul	Csa.1	Csa.1	Csa.2	Csa.3	Csa.4	Csa.6
Sfax	BWh.1	BWh.1	BWh.1	BWh.2	BWh.3	BWh.5
Siliana	Csa.2	Csa.3	Csa.4	Csa.5	Csa.6	Csa.7
Sousse	Csa.1	Csa.1	Csa.1	Csa.3	Csa.4	Csa.5
Sidi Bouzid	BWk.1	BWk.2	BWk.3	BWk.4	BWk.5	BWk.7
Tataouine	BWh.1	BWh.2	BWh.2	BWh.3	BWh.4	BWh.5
Tozeur	BWh.1	BWh.1	BWh.2	BWh.3	BWh.4	BWh.5
Tunis	Csa.1	Csa.1	Csa.2	Csa.3	Csa.4	Csa.6
Climate scale	1	2	3	4	5	6	7
HDD quantities	< 300	300–600	600–900	900–1200	1200–1500	1500–1800	> 1800

Table C8
New KGC sub-classifications based on CDDs base temperatures in Tunisia.

Cities	new KGC at 18 °C	new KGC at 20 °C	new KGC at 22 °C	new KGC at 24 °C	new KGC at 26 °C	new KGC at 28 °C
Bizerte	Csa.5	Csa.3	Csa.2	Csa.2	Csa.1	Csa.1
Gabes	BWh.6	BWh.5	BWh.3	BWh.2	BWh.2	BWh.1
Gafsa	BWh.6	BWh.4	BWh.3	BWh.2	BWh.2	BWh.1
Jendouba	Csa.4	Csa.3	Csa.2	Csa.2	Csa.1	Csa.1
Kebili	BWh.7	BWh.6	BWh.5	BWh.4	BWh.3	BWh.2
Le Kef	BSk.4	BSk.3	BSk.2	BSk.1	BSk.1	BSk.1
Kairouan	BSh.5	BSh.4	BSh.3	BSh.2	BSh.2	BSh.1
Kasserine	BSk.4	BSk.3	BSk.2	BSk.2	BSk.1	BSk.1
Medenine	BSh.6	BSh.5	BSh.3	BSh.2	BSh.2	BSh.1
Monastir	Bsh.5	Bsh.3	Bsh.2	Bsh.2	Bsh.1	Bsh.1
Nabeul	Csa.5	Csa.3	Csa.2	Csa.2	Csa.1	Csa.1
Sfax	BWh.5	BWh.4	BWh.3	BWh.2	BWh.1	BWh.1
Siliana	Csa.4	Csa.3	Csa.2	Csa.1	Csa.1	Csa.1
Sousse	Csa.5	Csa.3	Csa.2	Csa.2	Csa.1	Csa.1
Sidi Bouzid	BWk.5	BWk.4	BWk.3	BWk.2	BWk.1	BWk.1
Tataouine	BWh.7	BWh.6	BWh.4	BWh.4	BWh.3	BWh.2
Tozeur	BWh.7	BWh.6	BWh.4	BWh.4	BWh.3	BWh.2
Tunis	Csa.5	Csa.3	Csa.2	Csa.2	Csa.1	Csa.1
Climate scale	1	2	3	4	5	6	7
CDD quantities	< 300	300–600	600–900	900–1200	1200–1500	1500–1800	> 1800

Data availability

Data will be made available on request.

References

[1] D. Cui, S. Liang, D. Wang, Z. Liu, A 1-km global dataset of historical (1979–2017) and future (2020–2100) Köppen-Geiger climate classification and bioclimatic variables, Earth Syst. Sci. Data Discuss. 2021 (2021) 1–33.

[2] S. Hobbi, S.M. Papalexiou, C.R. Rajulapati, S.D. Nerantzaki, Y. Markonis, G. Tang, M.P. Clark, Detailed investigation of discrepancies in Köppen-Geiger climate classification using seven global gridded products, J. Hydrol. 612 (2022) 128121.

[3] T. Raziei, Climate of Iran according to Köppen-Geiger, Feddema, and UNEP climate classifications, Theor. Appl. Climatol. 148 (3) (2022) 1395–1416.

[4] Diggelmann, T., Boyd-Graber, J., Bulian, J., Ciaramita, M., & Leippold, M. (2020). Climate-fever: A dataset for verification of real-world climate claims. arXiv preprint arXiv:2012.00614.

[5] J. Rahimi, P. Laux, A. Khalili, Assessment of climate change over Iran: CMIP5 results and their presentation in terms of Köppen–Geiger climate zones, Theor. Appl. Climatol. 141 (2020) 183–199.

[6] X. Luo, P. Vahmani, T. Hong, A. Jones, City-scale building anthropogenic heating during heat waves, Atmos. 11 (11) (2020) 1206.

[7] Change, o. c., Intergovernmental panel on climate change, World Meteorological Organization 52 (2007) 1–43.

[8] S. Zhao, M. Liu, M. Tao, W. Zhou, X. Lu, Y. Xiong, Q. Wang, The role of satellite remote sensing in mitigating and adapting to global climate change. Science of the Total Environment, 2023.

[9] O. Hakam, A. Baali, K. Azennoud, A. Lyazidi, M. Bourchachen, Assessments of drought effects on plant production using satellite remote sensing technology, GIS and observed climate data in Northwest Morocco, case of the lower Sebou Basin, International Journal of Plant Production 17 (2) (2023) 267–282.

[10] M. Zargari, A. Mofidi, A. Entezari, M. Baaghideh, Climatic comparison of surface urban heat island using satellite remote sensing in Tehran and suburbs, Sci. Rep. 14 (1) (2024) 643.

[11] T.S. Pagano, V.H. Payne, The Atmospheric Infrared Sounder, in: Handbook of Air Quality and Climate Change, Singapore, Springer Nature Singapore, 2023, pp. 335–347.

[12] S. Karalis, E. Karymbalis, K. Tsanakas, Mid-Term Monitoring of Suspended Sediment Plumes of Greek Rivers Using Moderate Resolution Imaging Spectroradiometer (MODIS) Imagery, Remote Sens. (Basel) 15 (24) (2023) 5702.

[13] Ohara, K., Kubota, T., Kachi, M., & Kazumori, M. (2023). Comparison of long-term total precipitable water products by the Advanced Microwave Scanning Radiometer 2 (AMSR2). Journal of the Meteorological Society of Japan. Ser. II, 101 (4), 289-308.

[14] L. Wanchoo, F. Lindsay, D. Turcios, Y. Hao, H. Weir, December). NASA EOSDIS 20 Years of Data Usage and User Assessment in Support of Open Science Initiative No (2023).

[15] S. Fox, V. Mattioli, E. Turner, A. Vance, D. Cimini, D. Gallucci, An evaluation of atmospheric absorption models at millimetre and sub-millimetre wavelengths using airborne observations, Atmos. Meas. Tech. 17 (16) (2024) 4957–4978.

[16] Z.J. Zhai, J.M. Helman, Implications of climate changes to building energy and design, Sustain. Cities Soc. 44 (2019) 511–519.

[17] L.M. Campagna, F. Fiorito, On the impact of climate change on building energy consumptions: a meta-analysis, Energies 15 (1) (2022) 354.

[18] J. Huang, K.R. Gurney, The variation of climate change impact on building energy consumption to building type and spatiotemporal scale, Energy 111 (2016) 137–153.

[19] B. Omarov, S.A. Memon, J. Kim, A novel approach to develop climate classification based on degree days and building energy performance, Energy 267 (2023) 126514.

[20] Pangsy-Kania, S., Biegańska, J., Flouros, F., & Sokół, A. (2024). Heating and cooling degree-days vs climate change in years 1979-2021. Evidence from the European Union and Norway. Ekonomia i Środowisko, 88(1).

[21] R.D. Figaj, D.M. Laudiero, A. Mauro, Climate Characterization and Energy Efficiency in Container Housing: Analysis and Implications for Container House Design in European Locations, Energies 17 (12) (2024) 2926.

[22] J. Song, Y. Lu, T. Fischer, K. Hu, Effects of the urban landscape on heatwave-mortality associations in Hong Kong: comparison of different heatwave definitions, Front. Environ. Sci. Eng. 18 (1) (2024) 11.

[23] J. Spinoni, J.V. Vogt, P. Barbosa, A. Dosio, N. McCormick, A. Bigano, H.M. Füssel, Changes of heating and cooling degree-days in Europe from 1981 to 2100, Int. J. Climatol 38 (51) (2018) e191–e208.

[24] Y. Petri, K. Caldeira, Impacts of global warming on residential heating and cooling degree-days in the United States, Sci. Rep. 5 (1) (2015) 12427.

[25] C. Xu, G. Huang, M. Zhang, Comparative analysis of the seasonal driving factors of the urban heat environment using machine learning: evidence from the wuhan urban agglomeration, China, 2020, Atmos. 15 (6) (2024) 671.

[26] C. Hu, M. Zhang, G. Huang, Z. Li, Y. Sun, J. Zhao, Tracking the impact of the land cover change on the spatial-temporal distribution of the thermal comfort: Insights from the Qinhuai River Basin, China. Sustainable Cities and Society 116 (2024) 105916.

[27] A.o. Wang, M. Zhang, E. Chen, C. Zhang, Y. Han, Impact of seasonal global land surface temperature (LST) change on gross primary production (GPP) in the early 21st century, Sustain. Cities Soc. 110 (2024) 105572.

[28] M. Zhang, S. Tan, C. Zhang, S. Han, S. Zou, E. Chen, Assessing the impact of fractional vegetation cover on urban thermal environment: A case study of Hangzhou, China. Sustainable Cities and Society 96 (2023) 104663.

[29] H. Filahi, H. Omrani, S. Claudel, P. Drobinski, Temporal fragmentation of the energy demand in Europe: Impact of climate change on the maneuverability of energy system, Clim. Serv. 34 (2024) 100469.

[30] A. Karagiannidis, K. Lagouvardos, V. Kotroni, E. Galanaki, Expected changes in heating and cooling degree days over Greece in the near future based on climate scenarios projections, Atmos. 15 (4) (2024) 393.

[31] E.A. Grigorieva, A. Matzarakis, C.R. De Freitas, Analysis of growing degree-days as a climate impact indicator in a region with extreme annual air temperature amplitude, Climate Res. 42 (2) (2010) 143–154.

[32] A. Matzarakis, D. Ivanova, C. Balafoutis, T. Makrogiannis, Climatology of growing degree days in Greece, Climate Res. 34 (3) (2007) 233–240.

[33] C. Liddell, C. Morris, Fuel poverty and human health: a review of recent evidence, Energy Policy 38 (6) (2010) 2987–2997.

[34] S. Attia, C. Gobin, Climate change effects on Belgian households: a case study of a nearly zero energy building, Energies 13 (20) (2020) 5357.

[35] M. Taleghani, M. Tenpierik, S. Kurvers, A. Van Den Dobbelsteen, A review into thermal comfort in buildings, Renew. Sustain. Energy Rev. 26 (2013) 201–215.

[36] C.S.G. Sánchez, A. Mavrogianni, F.J.N. González, On the minimal thermal habitability conditions in low income dwellings in Spain for a new definition of fuel poverty, Build. Environ. 114 (2017) 344–356.

[37] T. Tabata, P. Tsai, Fuel poverty in Summer: An empirical analysis using microdata for Japan, Sci. Total Environ. 703 (2020) 135038.

[38] E.H.M. Bah, I. Faye, Z.F. Geh, Housing market dynamics in Africa, Springer Nature, 2018.

[39] J. Gbadegesin, L. Marais, The state of housing policy research in Africa, Int. J. Hous. Policy 20 (4) (2020) 474–490.

[40] M. Huchzermeyer, A. Karam (Eds.), Informal Settlements: A Perpetual Challenge?, Juta and Company Ltd., 2006.

[41] B.O. Ganiyu, J.A. Fapohunda, R. Haldenwang, Sustainable housing financing model to reduce South Africa housing deficit, International Journal of Housing Markets and Analysis 10 (3) (2017) 410–430.

[42] L. Strohmenger, L. Collet, V. Andréassian, L. Corre, F. Rousset, G. Thirel, Köppen–Geiger climate classification across France based on an ensemble of high-resolution climate projections, Comptes Rendus. Géoscience 356 (G1) (2024) 67–82.

[43] C. Andrade, J.A. Santos, A. Fonseca, Worldwide Köppen Geiger Climate Classification Changes Projections (SSP2-2.6 and SSP5-8.5), No. EMS2023-336, Copernicus Meetings, 2023.

[44] A. Valjarević, M. Milanović, I. Gultepe, D. Filipović, T. Lukić, Updated Trewartha climate classification with four climate change scenarios, Geogr. J. 188 (4) (2022) 506–517.

[45] N. Phumkokrux, P. Trivej, Investigation of Temperature, Precipitation, Evapotranspiration, and New Thornthwaite Climate Classification in Thailand, Atmos. 15 (3) (2024) 379.

[46] K.L. McCurley Pisarello, J.W. Jawitz, Coherence of global hydroclimate classification systems, Hydrol. Earth Syst. Sci. 25 (12) (2021) 6173–6183.

[47] L.M. Al-Hadhrami, Comprehensive review of cooling and heating degree days characteristics over Kingdom of Saudi Arabia, Renew. Sustain. Energy Rev. 27 (2013) 305–314.

[48] K.P. Amber, M.W. Aslam, F. Ikram, A. Kousar, H.F. Ali, N. Akram, H. Mushtaq, Heating and cooling degree-days maps of Pakistan, Energies 2018 (11) (2018) 94.

[49] W.A. Mahar, G. Verbeeck, M.K. Singh, S. Attia, An investigation of thermal comfort of houses in dry and semi-arid climates of Quetta, Pakistan. Sustainability 11 (19) (2019) 5203.

[50] J. Spinoni, J. Vogt, P. Barbosa, European degree-day climatologies and trends for the period 1951-2011, Int. J. Climatol. 35 (1) (2015).

[51] B. Möller, E. Wiechers, U. Persson, L. Grundahl, D. Connolly, Heat Roadmap Europe: Identifying local heat demand and supply areas with a European thermal atlas, Energy 158 (2018) 281–292.

[52] A. Janković, Z. Podraščanin, V. Djurdjevic, Future climate change impacts on residential heating and cooling degree days in Serbia, IDŐJÁRÁS/QUARTERLY JOURNAL OF THE HUNGARIAN METEOROLOGICAL SERVICE 123 (3) (2019) 351–370.

[53] F. Azimi, R. Ebrahimi, M. Narangifard, Analysis and mapping of the HDD, CDD and temperatures for southern Caspian Sea Based Model EH5OM, International Journal of Urban Management and Energy Sustainability 1 (4) (2020) 1–11.

[54] C. Andrade, S. Mourato, J. Ramos, Heating and cooling degree-days climate change projections for Portugal, Atmos. 12 (6) (2021) 715.

[55] N.A. Fry, Building-level heat demand mapping of commercial-residential areas for simulated district heating assessments in Montana, Idaho, and Washington, Energ. Buildings 245 (2021) 111075.

[56] Y. Li, J. Li, A. Xu, Z. Feng, C. Hu, G. Zhao, Spatial-temporal changes and associated determinants of global heating degree days, Int. J. Environ. Res. Public Health 18 (12) (2021) 6186.

[57] N.D. Miranda, J. Lizana, S.N. Sparrow, M. Zachau-Walker, P.A. Watson, D. C. Wallom, M. McCulloch, Change in cooling degree days with global mean temperature rise increasing from 1.5 C to 2.0 C, Nat. Sustainability 6 (11) (2023) 1326–1330.

[58] R. Idchabani, M. Garoum, A. Khaldoun, Analysis and mapping of the heating and cooling degree-days for Morocco at variable base temperatures, Int. J. Ambient Energy 36 (4) (2015) 190–198.

[59] D. Conradie, T. van Reenen, S. Bole, Degree-day building energy reference map for South Africa, Build. Res. Inf. 46 (2) (2018) 191–206.

[60] S. Semahi, M.A. Benbouras, W.A. Mahar, N. Zemmouri, S. Attia, Development of spatial distribution maps for energy demand and thermal comfort estimation in Algeria, Sustainability 12 (15) (2020) 6066.

[61] Dicko, K., Umaru, E. T., Sanogo, S., Okhimamhe, A. A., & Löwner, R. (2024). Long-term analysis of changes in cooling degree-days in West Africa under global warming.

[62] E. Guilyardi, El Niño–mean state–seasonal cycle interactions in a multi-model ensemble, Clim. Dyn. 26 (2006) 329–348.

[63] O. Büyükalaca, H. Bulut, T. Yılmaz, Analysis of variable-base heating and cooling degree-days for Turkey, Appl. Energy 69 (4) (2001) 269–283.
[64] NASA POWER | Prediction Of Worldwide Energy Resources: https://power.larc.nasa.gov/. Accessed on 15th November 2024.
[65] S.S. Abolhassani, M.M. Joybari, M. Hosseini, M. Parsaee, U. Eicker, A systematic methodological framework to study climate change impacts on heating and cooling demands of buildings, Journal of Building Engineering 63 (2023) 105428.
[66] Climatic Data for Building Design Standards: https://www.ashrae.org/continuous-maintenance.
[67] Climate.OneBuilding.Org: https://climate.onebuilding.org/. Accessed on 25th October 2024.
[68] MECHRI, H. E., CORRADO, V., & GANNAR, M. Z. (2007). Building Energy labeling in Tunisia. In Conference Climamed: Genoa, Italy.
[69] A.A. Saleem, A.K. Abel-Rahman, A.H.H. Ali, S. Ookawara, An analysis of thermal comfort and energy consumption within public primary schools in Egypt. IAFOR J. Sustain, Energy Environ 3 (2016).
[70] N. El Asri, N. Abdou, M. Mharzi, A. Maghnouj, Moroccan Public Buildings and the RTCM: Insights into Compliance, Energy Performance, and Regulation Improvement, Energies 16 (18) (2023) 6496.
[71] World Population Review: https://worldpopulationreview.com/. Accessed on 16th August 2024.
[72] A.H. Sparks, nasapower: a NASA POWER global meteorology, surface solar energy and climatology data client for R, Journal of Open Source Software 3 (30) (2018) 1035.
[73] H. Aboelkhair, M. Morsy, G. El Afandi, Assessment of agroclimatology NASA POWER reanalysis datasets for temperature types and relative humidity at 2 m against ground observations over Egypt, Adv. Space Res. 64 (1) (2019) 129–142.
[74] J.W. White, G. Hoogenboom, P.W. Wilkens, P.W. Stackhouse Jr, J.M. Hoel, Evaluation of satellite-based, modeled-derived daily solar radiation data for the continental United States, Agron. J. 103 (4) (2011) 1242–1251.
[75] Y.C. Duarte, P.C. Sentelhas, NASA/POWER and DailyGridded weather datasets—how good they are for estimating maize yields in Brazil? Int. J. Biometeorol. 64 (2020) 319–329.
[76] M. Bhatnagar, J. Mathur, V. Garg, Determining base temperature for heating and cooling degree-days for India, Journal of Building Engineering 18 (2018) 270–280.
[77] L.D. Harvey, Using modified multiple heating-degree-day (HDD) and cooling-degree-day (CDD) indices to estimate building heating and cooling loads, Energ. Buildings 229 (2020) 110475.
[78] R. Athalye, T. Taylor, B. Liu, Impact of ASHRAE Standard 169-2013 on building energy codes and energy efficiency, Proceedings of SimBuild 6 (1) (2016).
[79] C. Childs, Interpolating surfaces in ArcGIS spatial analyst, ArcUser, July-September 3235 (569) (2004) 32–35.
[80] A. Sadeqi, H. Tabari, Y. Dinpashoh, Spatio-temporal analysis of heating and cooling degree-days over Iran, Stoch. Env. Res. Risk A. (2022) 1–23.
[81] Li, J., & Heap, A. D. (2008). A review of spatial interpolation methods for environmental scientists.
[82] T. Wu, Y. Li, Spatial interpolation of temperature in the United States using residual kriging, Appl. Geogr. 44 (2013) 112–120.
[83] M.R. Holdaway, Spatial modeling and interpolation of monthly temperature using kriging, Climate Res. 6 (3) (1996) 215–225.
[84] K. Malcheva, L. Bocheva, T. Marinova, Mapping temperature and precipitation climate normals over Bulgaria by using ArcGIS Pro 2.4, Bulg. J. Meteorol. Hydrol 2 (2020) 61–77.
[85] S. Abebe, T. Assefa, Determining and mapping the base temperature for heating and cooling degree days for Ethiopia, Energ. Effi. 15 (8) (2022) 62.